

Ringberg Workshop

New Trends in HERA Physics 2008

October 5 - 10, 2008

Ringberg Castle, Tegernsee



Jet substructure at HERA

C Glasman
Universidad Autónoma de Madrid



from

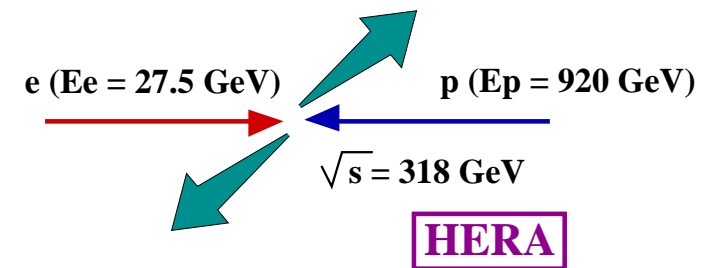
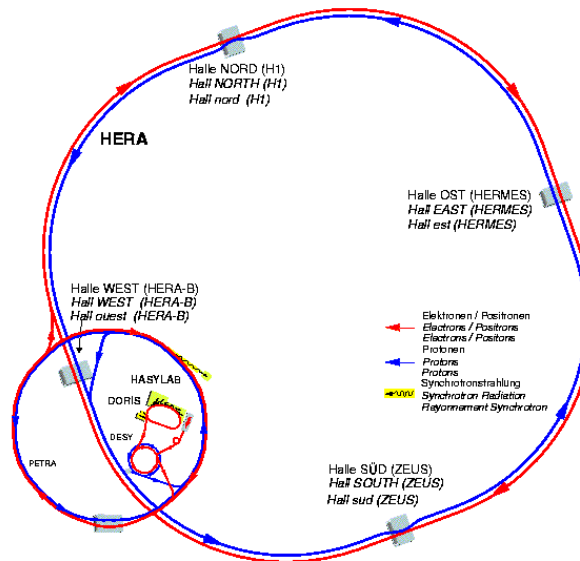


ZEUS Collab.

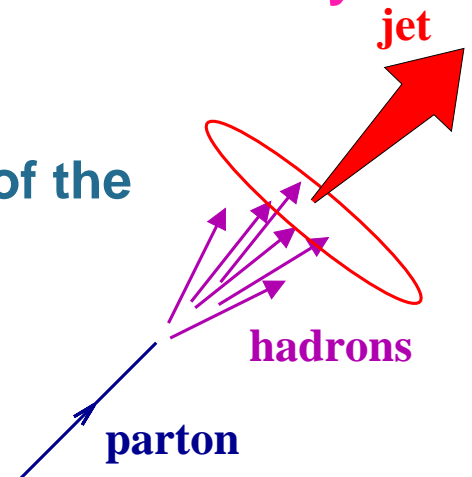


H1 Collab.

at

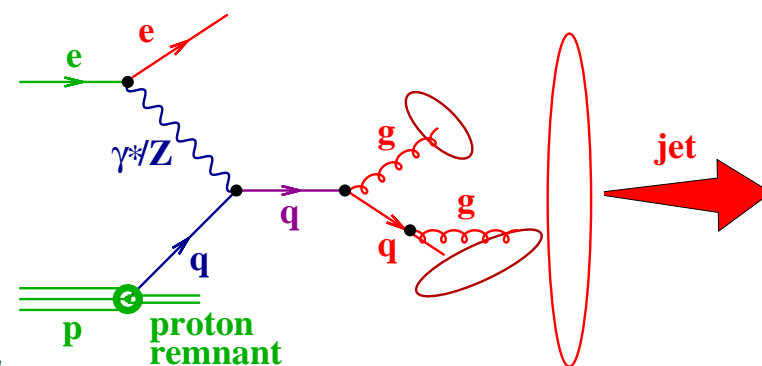


Jets and jet structure

- **Perturbative calculations lead to partonic final states which are not directly accessible to the experimentalist**
 - hadrons and not partons are observed in the final state
 - the observed hadrons are the result of the fragmentation of the coloured partons
 - all hadrons originating from a parton are contained in a narrow region around the original parton direction of motion, forming a “jet”
- 
- The first step in comparing experimental results with theoretical calculations is to group hadrons into jets to recover the parton topology (jet algorithms)
- **Jet structure:**
 - the p_L distribution of the hadrons in a jet scales with jet energy
 - the p_T distribution of the hadrons in a jet has a mean value of ~ 300 MeV
 - p_T/p_L (mean angle between a hadron and the jet axis) should decrease with jet energy → the size of a cone which contains a constant fraction of jet energy decreases with the jet energy
 - at high energies, gluon emission dominates and fragmentation effects become negligible → structure of jets driven by radiation and calculable in pQCD

Jet substructure

- The investigation of the **internal structure of jets** gives insight into the **transition** between a **parton** produced in a hard process and the experimentally observable jet of hadrons
- **QCD predictions:**
 - jet substructure driven by **gluon emission** off primary partons (at sufficiently **high E_T^{jet}** , fragmentation effects negligible)
 - **gluon jets** are **broader** than **quark jets** (larger colour charge of the gluon)
 - jet substructure depends mainly on **flavour** of primary parton from which the jet originated and to a lesser extent on the **hard scattering process**



Jet substructure: integrated jet shape

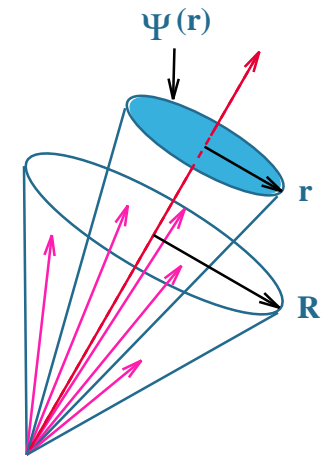
- $\psi(r)$: fraction of the jet transverse energy that lies inside a cone in the $\eta - \varphi$ plane of radius r , concentric with the jet axis

$$\psi(r) = \frac{E_T(r)}{E_T^{\text{jet}}}$$

→

$$\langle \psi(r) \rangle = \frac{1}{N_{\text{jets}}} \sum_{\text{jets}} \frac{E_T(r)}{E_T^{\text{jet}}}$$

mean integrated jet shape



Jet substructure: subjet multiplicity

- **subjets**: are resolved within a jet by reapplying the k_T cluster algorithm until for every pair of particles i, j

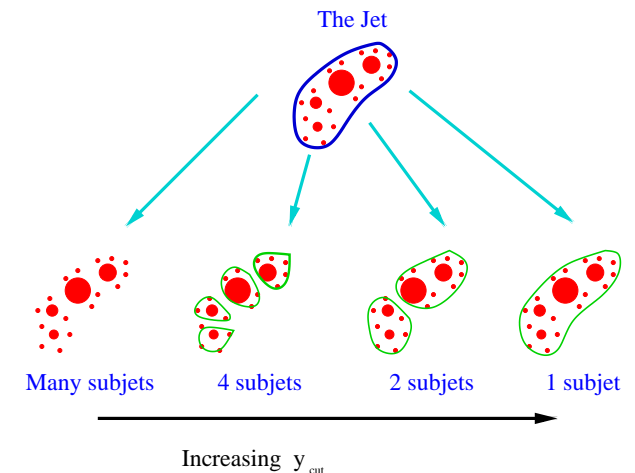
$$d_{ij} = \min(E_{Ti}, E_{Tj})^2 [(\eta_i - \eta_j)^2 + (\varphi_i - \varphi_j)^2]$$

is above $y_{\text{cut}} \cdot (E_T^{\text{jet}})^2$

→

$$\langle n_{\text{sbj}}(y_{\text{cut}}) \rangle = \frac{1}{N_{\text{jets}}} \sum_{i=1}^{N_{\text{jets}}} n_{\text{sbj}}^i(y_{\text{cut}})$$

mean subjet multiplicity



QCD calculations of jet substructure

- **QCD-based Monte Carlo models:**

→ PYTHIA, HERWIG, ARIADNE, LEPTO approximate the substructure of jets with parton showers

- **Fixed-order QCD calculations:**

→ at lowest order, a jet consists of one parton (no structure)

→ higher-order terms give the non-trivial contributions

→ **NLO** calculations in NC DIS are possible in **LAB** frame from $\mathcal{O}(\alpha_s^2)$ predictions since **three partons** can be inside one jet

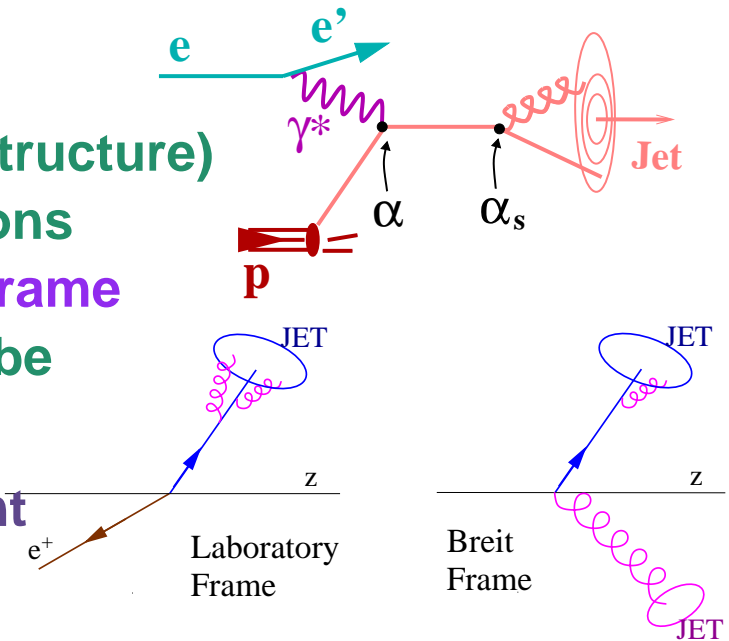
- **Measurements of jet substructure provide a stringent test of pQCD calculations directly beyond LO**

- **pQCD calculations of jet shapes:**

$$\langle 1 - \psi(r) \rangle = \frac{\int_r^R dE_T (E_T/E_T^{\text{jet}}) [d\sigma(ep \rightarrow 2\text{partons})/dE_T]}{\sigma_{\text{jet}}(E_T^{\text{jet}})}$$

- **pQCD calculations of subjet multiplicities:**

$$\langle n_{\text{subj}}(y_{\text{cut}}) \rangle = 1 + \frac{1}{\sigma_{\text{jet}}} \sum_{j=2}^{\infty} (j-1) \cdot \sigma_{\text{subj},j}(y_{\text{cut}}) = 1 + C_1 \alpha_s + C_2 \alpha_s^2$$

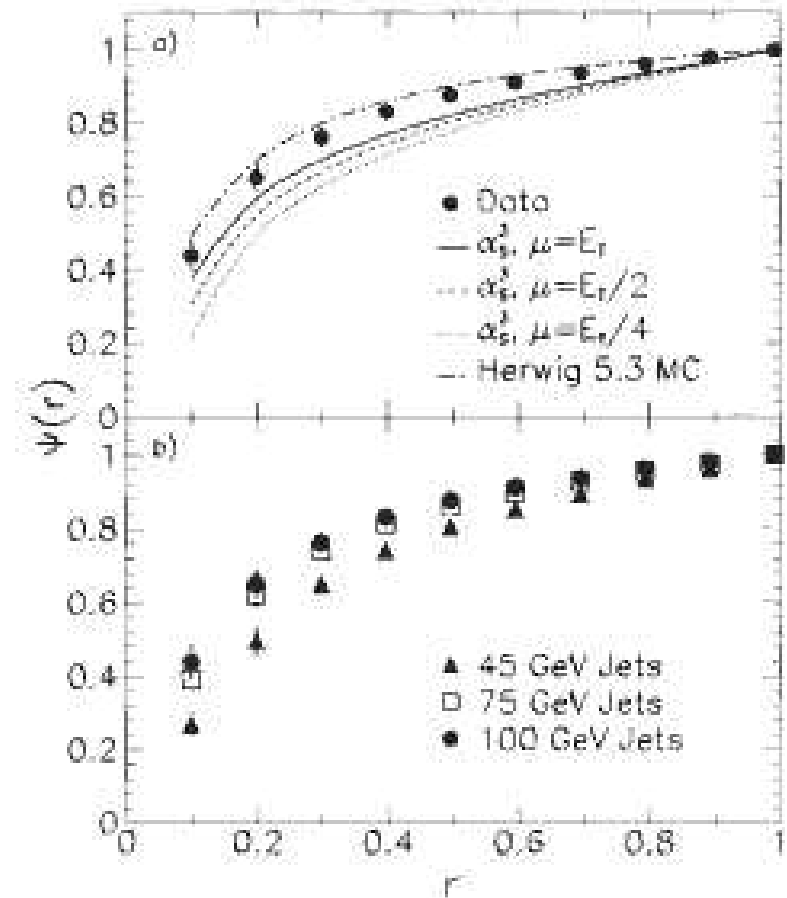


Jet substructure and QCD predictions

- **QCD predictions:**

→ jet substructure driven by **gluon emission** off primary partons (at sufficiently **high** E_T^{jet} , fragmentation effects negligible)

- **Adequate description of data by $\mathcal{O}(\alpha_s^3)$ theory and QCD-based MC models**
- **QCD prediction confirmed!**



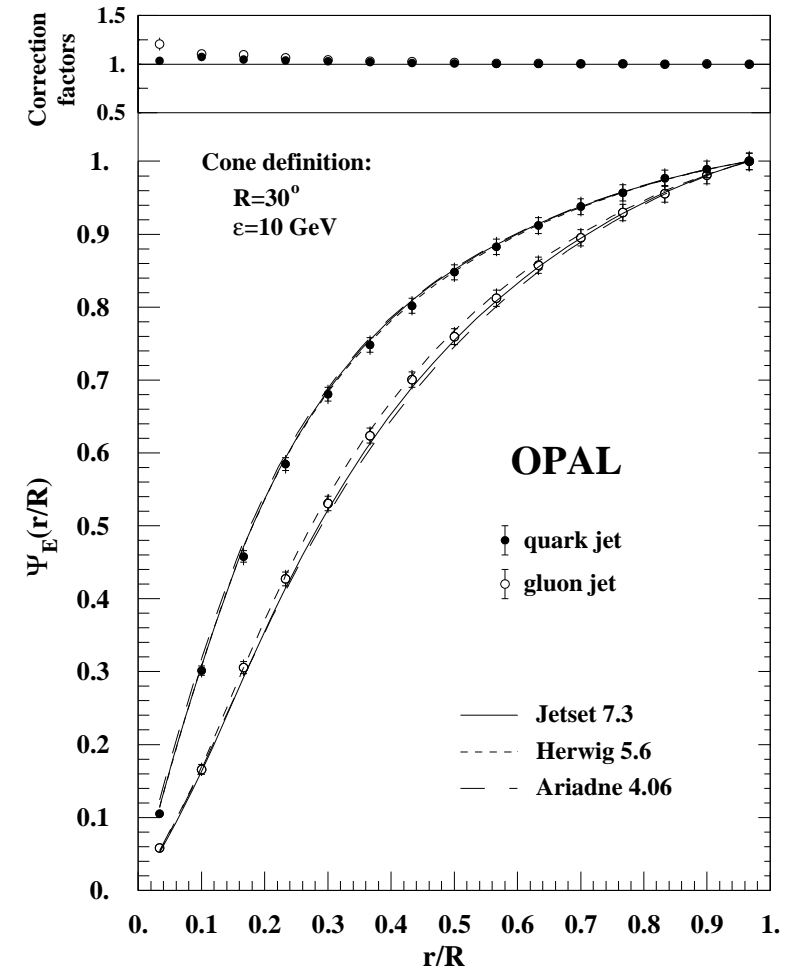
Jet substructure and QCD predictions

- **QCD predictions:**

→ **gluon jets are broader than quark jets (larger colour charge of the gluon)**

→ **Gluon jets are seen to be substantially broader than quark jets**

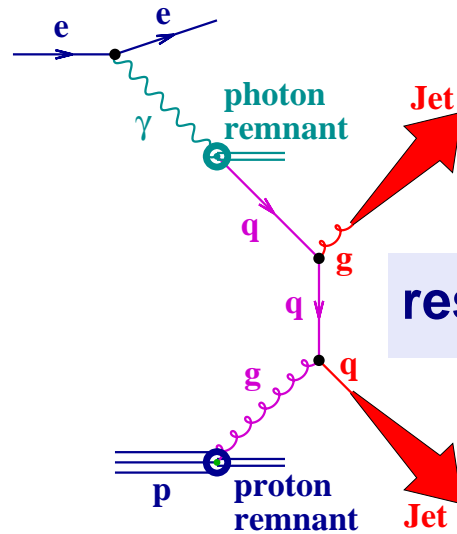
→ **QCD prediction confirmed!**



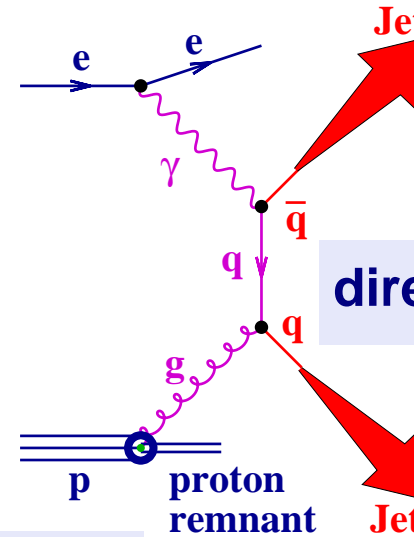
Tests of pQCD using jet substructure at HERA

Jet production at HERA

- Jet production in photoproduction up to $\mathcal{O}(\alpha_s)$:



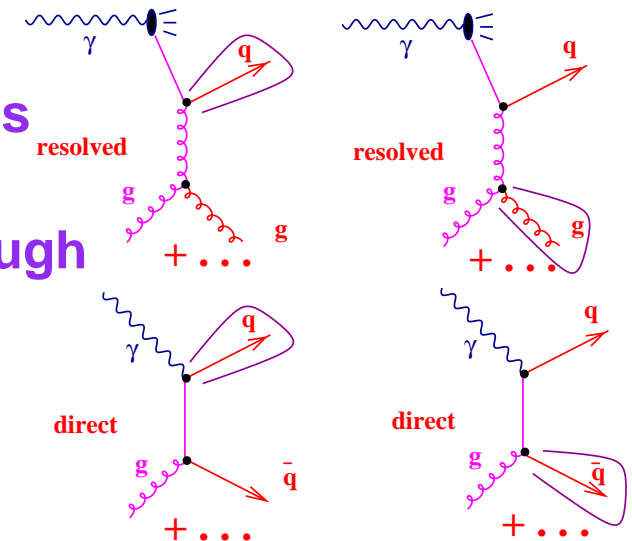
resolved: $x_\gamma^{obs} < 1$



direct: $x_\gamma^{obs} \sim 1$

$$x_\gamma^{obs} = \frac{1}{E_\gamma} (\sum_{jets} E_T^{jet} e^{-\eta^{jet}})$$

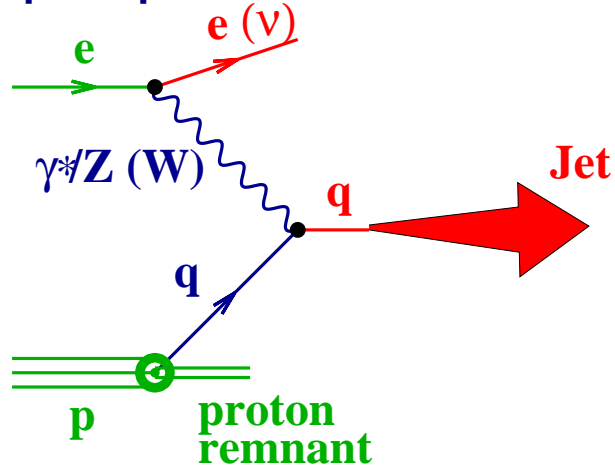
- resolved processes give rise to quark and gluon jets through $q\gamma g p \rightarrow qg, g\gamma g p \rightarrow gg, \dots$
- direct processes give rise mostly to quark jets through $\gamma g \rightarrow q\bar{q}$
- η^{jet} dependence of jet substructure expected to show quark-like jets for $\eta^{jet} < 0$ and gluon-like jets in forward direction due to HERA dynamics



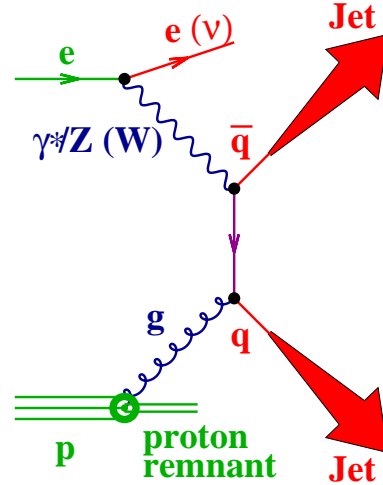
Jet production at HERA

- Jet production in neutral and charged current deep inelastic ep scattering up to $\mathcal{O}(\alpha_s)$:

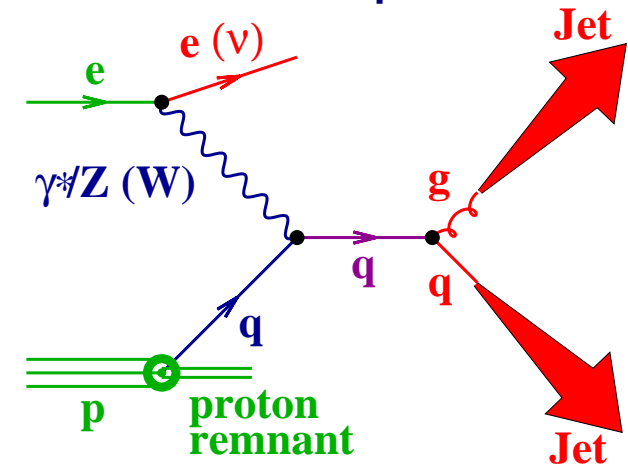
quark-parton model



boson-gluon fusion



QCD Compton



- Inclusive-jet sample expected to be dominated by quark jets
 - no dependence of jet substructure on η^{jet} expected
- Dijet sample expected to contain a larger fraction of gluon jets
 - jets expected to become broader as η^{jet} increases

Mean integrated jet shape in photoproduction



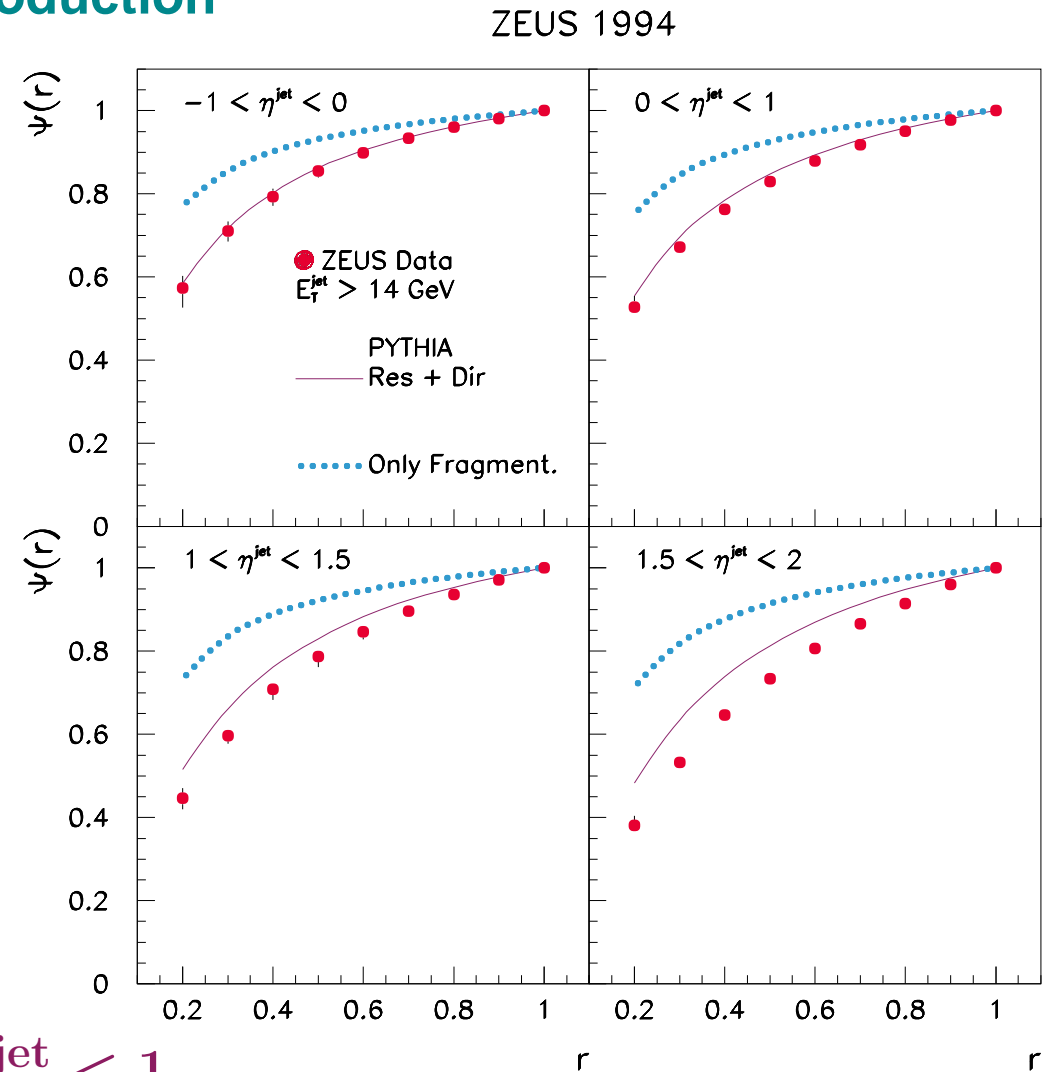
• η^{jet} dependence of $\langle\psi(r)\rangle$ in photoproduction

- Jets searched using the cone algorithm
- Kinematic region: $0.2 < y < 0.85$ and $Q^2 \leq 4 \text{ GeV}^2$
- At least one jet with $E_T^{\text{jet}} > 14 \text{ GeV}$ and $-1 < \eta^{\text{jet}} < 2$

- $\langle\psi(r)\rangle$ vs r in different η^{jet} regions:
 - jets become broader as η^{jet} increases

• Comparison to QCD predictions:

- models with only fragmentation predict jets too narrow
- models including initial- and final-state QCD radiation give a good description of the data for $-1 < \eta^{\text{jet}} < 1$
- parton radiation dominant mechanism responsible for jet shape



Mean integrated jet shape in photoproduction



• η^{jet} dependence of $\langle \psi(r) \rangle$ in photoproduction

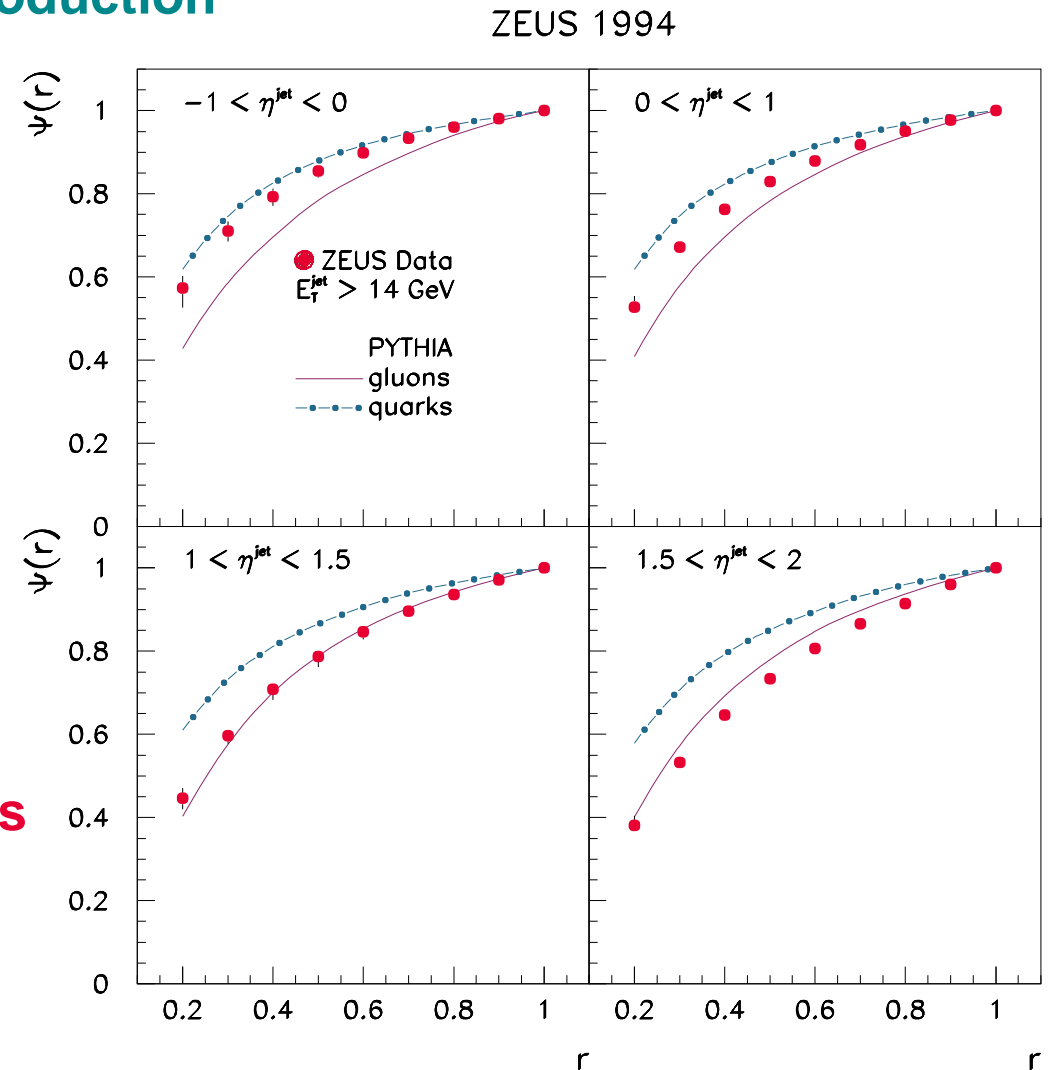
- Jets searched using the cone algorithm
- Kinematic region: $0.2 < y < 0.85$ and $Q^2 \leq 4 \text{ GeV}^2$
- At least one jet with $E_T^{\text{jet}} > 14 \text{ GeV}$ and $-1 < \eta^{\text{jet}} < 2$

• $\langle \psi(r) \rangle$ vs r in different η^{jet} regions:

→ jets become broader as η^{jet} increases

• Comparison to QCD predictions:

- predictions for gluon and quark jets show that the measured jets are
 - quark-like for $-1 < \eta^{\text{jet}} < 0$
 - gluon-like for $1 < \eta^{\text{jet}} < 2$



Mean integrated jet shape in photoproduction



• η^{jet} and E_T^{jet} dependence of $\langle \psi(r=0.5) \rangle$ in photoproduction

– Jets searched using the k_T cluster algorithm

– Kinematic region: $0.2 < y < 0.85$ and

$$Q^2 \leq 1 \text{ GeV}^2$$

– At least one jet with $E_T^{\text{jet}} > 17 \text{ GeV}$ and

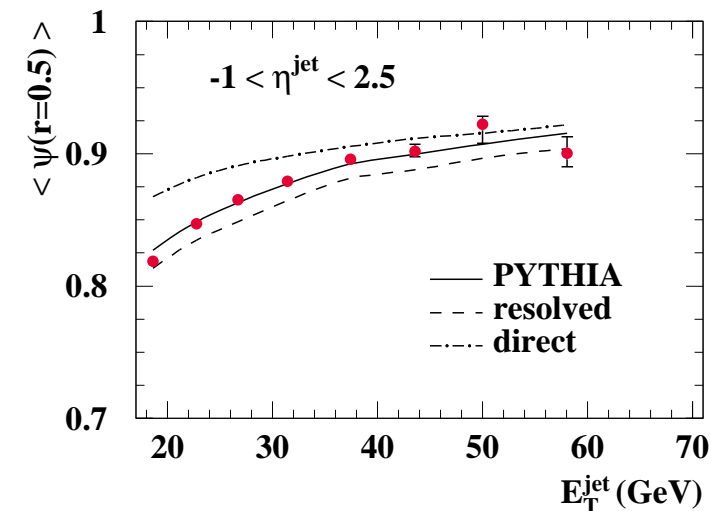
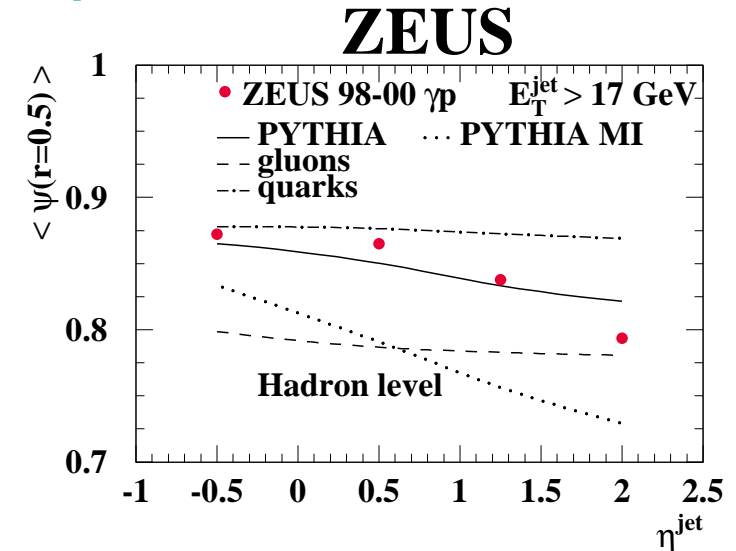
$$-1 < \eta^{\text{jet}} < 2.5$$

• The measured $\langle \psi(r=0.5) \rangle$ decreases with η^{jet}
 → the jets become broader as η^{jet} increases

• The measured $\langle \psi(r=0.5) \rangle$ increases with E_T^{jet}
 → the jets become narrower as E_T^{jet} increases

• Comparison with the predictions for gluon and quark jets:

→ the broadening of the jets is consistent with an increasing fraction of gluon jets as η^{jet} increases





Mean integrated jet shape in photoproduction

- x_γ^{obs} and η^{jet} dependence of $\langle\psi(r)\rangle$ in photoproduction

- Jets searched using the k_T cluster algorithm

- Kinematic region: $0.2 < y < 0.8$ and

$$Q^2 \leq 1 \text{ GeV}^2$$

- At least two jets with $E_T^{\text{jet}} > 7, 6 \text{ GeV}$ and

$$-0.75 < \eta^{\text{jet}} < 1.5$$

- $\langle\psi(r)\rangle$ vs r in different x_γ^{obs} regions:

- jets for $x_\gamma^{\text{obs}} \leq 0.75$ are broader than for $x_\gamma^{\text{obs}} > 0.75$

- $\langle\psi(r=0.5)\rangle$ decreases with η^{jet}

- jets become broader as η^{jet} increases

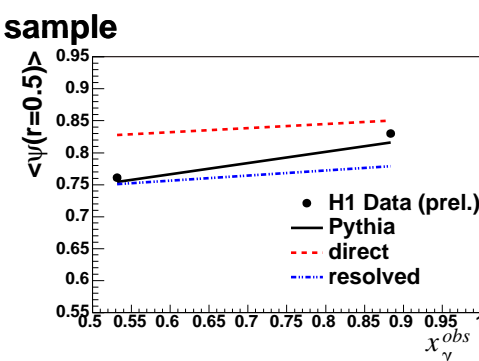
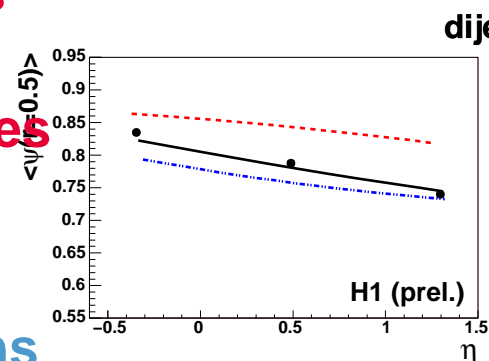
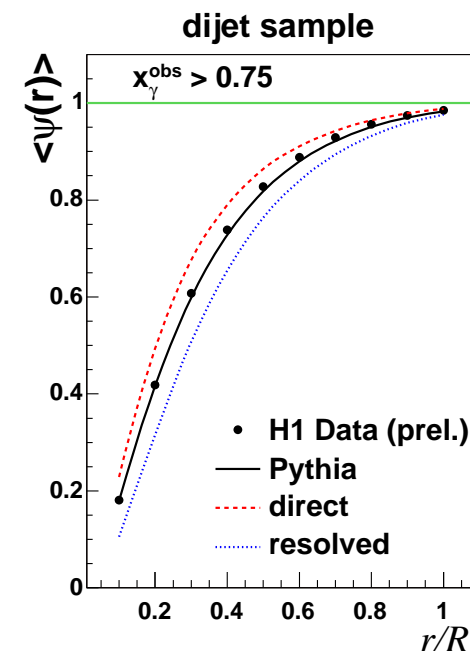
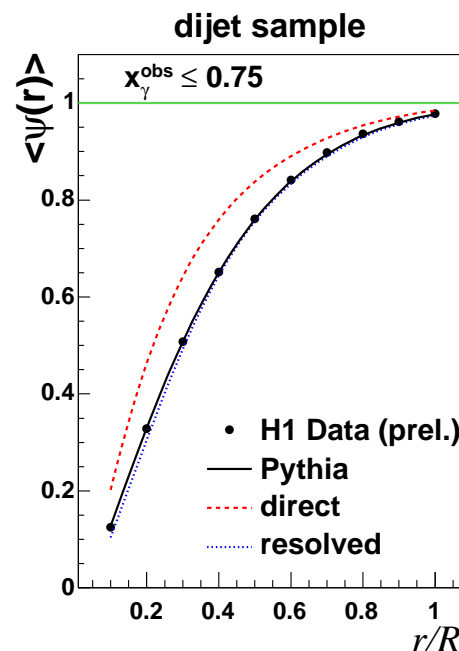
- $\langle\psi(r=0.5)\rangle$ increases with x_γ^{obs}

- jets become narrower as x_γ^{obs} increases

- Comparison to QCD predictions for resolved and direct:

- good description of data by predictions

- data consistent with being dominated by resolved for $x_\gamma^{\text{obs}} \leq 0.75$ and by direct for $x_\gamma^{\text{obs}} > 0.75$





Mean integrated jet shape in NC DIS

- r , η_B^{jet} and $E_{T,B}^{\text{jet}}$ dependence of $\langle \psi(r) \rangle$ in NC DIS

- Jets searched using the k_T cluster algorithm in Breit frame

- Kinematic region: $10 < Q^2 < 120 \text{ GeV}^2$

- At least two jets with $E_{T,B}^{\text{jet}} > 5 \text{ GeV}$ and $-1 < \eta_{\text{LAB}}^{\text{jet}} < 2$

- The measured $\langle \psi(r=0.5) \rangle$ decreases with η_B^{jet}
 - the jets become broader towards proton direction
 - effect more pronounced at low $E_{T,B}^{\text{jet}}$

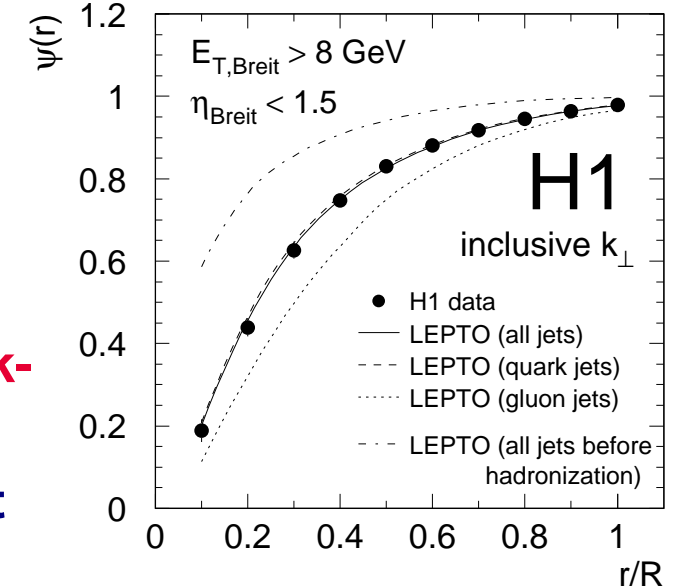
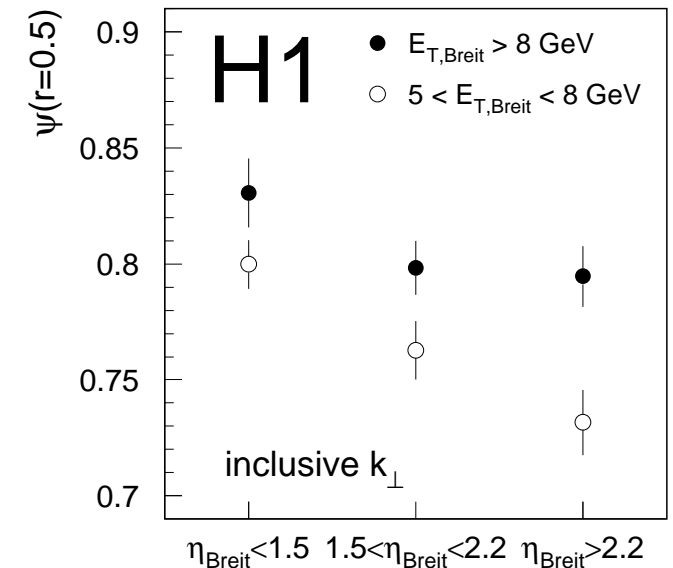
- The measured $\langle \psi(r=0.5) \rangle$ increases with $E_{T,B}^{\text{jet}}$
 - the jets become narrower as $E_{T,B}^{\text{jet}}$ increases

- Comparison to QCD predictions:

- the data are well described by the QCD-based MC models

- MC models predict jet sample dominated by quark-initiated jets

- observed jet substructure compatible with that of quark-initiated jets



H1 Collab, NP B 545 (1999) 3



Mean integrated jet shape in NC DIS

• η^{jet} dependence of $\langle \psi(r) \rangle$ in NC DIS

– Jets searched using the k_T cluster algorithm in LAB frame

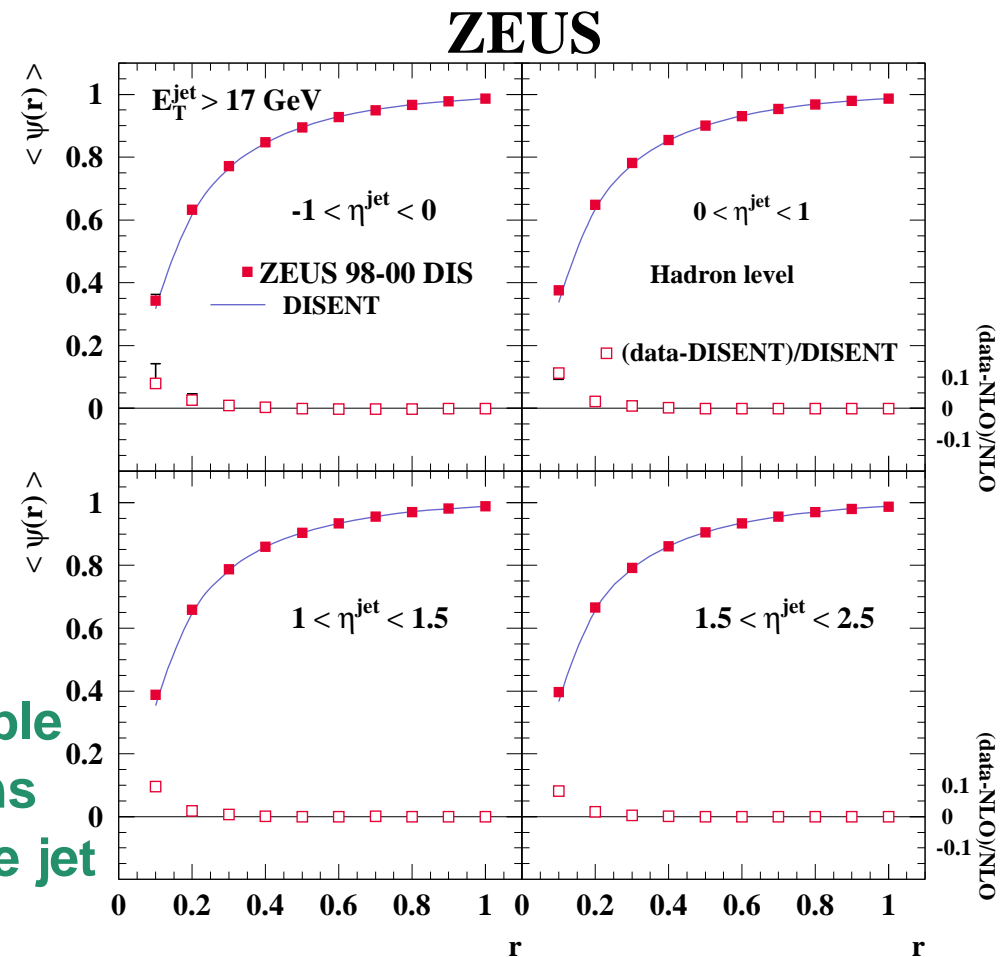
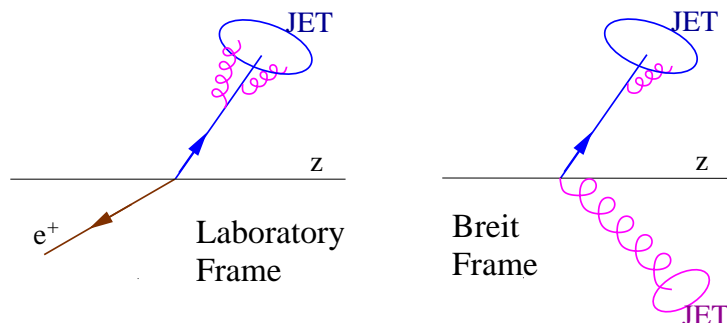
– Kinematic region: $Q^2 > 125 \text{ GeV}^2$

– At least one jet with $E_T^{\text{jet}} > 17 \text{ GeV}$ and $-1 < \eta^{\text{jet}} < 2.5$

• $\langle \psi(r) \rangle$ vs r in different η^{jet} regions:
 → no significant variation with η^{jet} is observed

• Comparison to QCD predictions:

→ NLO predictions in NC DIS are possible in LAB frame from $\mathcal{O}(\alpha_s^2)$ calculations since three partons can be inside one jet



→ the data are well described by the NLO QCD calculations for $r > 0.1$



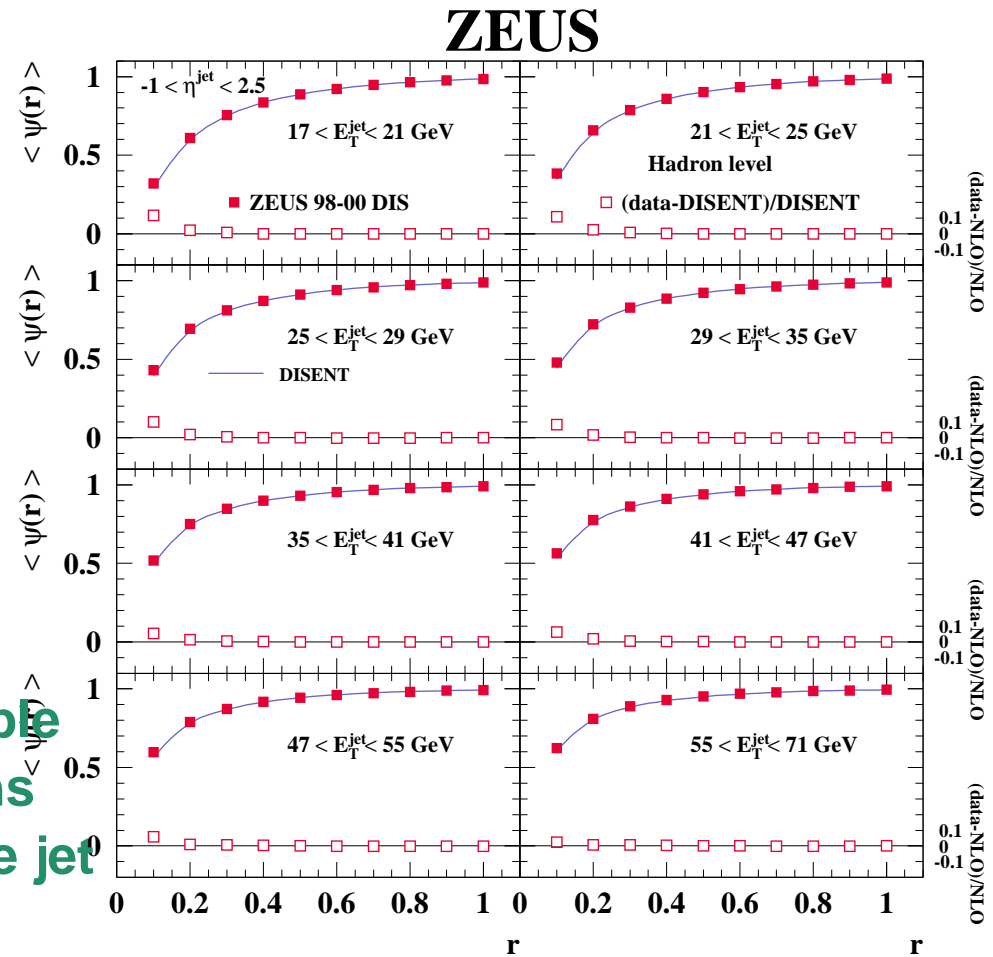
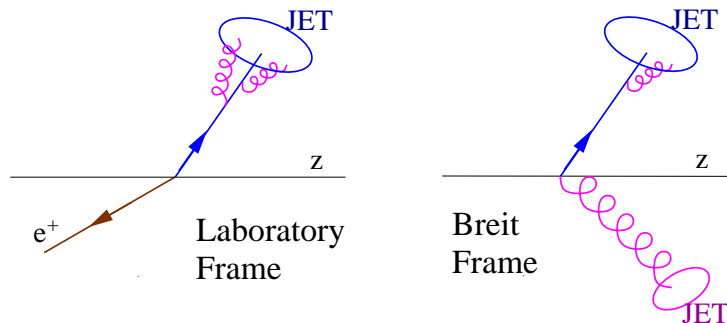
Mean integrated jet shape in NC DIS

- E_T^{jet} dependence of $\langle \psi(r) \rangle$ in NC DIS

- Jets searched using the k_T cluster algorithm in LAB frame
- Kinematic region: $Q^2 > 125 \text{ GeV}^2$
- At least one jet with $E_T^{\text{jet}} > 17 \text{ GeV}$ and $-1 < \eta^{\text{jet}} < 2.5$

- $\langle \psi(r) \rangle$ vs r in different E_T^{jet} regions:
 - the jets become narrower as E_T^{jet} increases

- Comparison to QCD predictions:
 - NLO predictions in NC DIS are possible in LAB frame from $\mathcal{O}(\alpha_s^2)$ calculations since three partons can be inside one jet



→ the data are well described by the NLO QCD calculations for $r > 0.1$

Mean integrated jet shape in NC DIS



• η^{jet} and E_T^{jet} dependence of $\langle \psi(r=0.5) \rangle$ in NC DIS

– Jets searched using the k_T cluster algorithm in LAB frame

– Kinematic region: $Q^2 > 125 \text{ GeV}^2$

– At least one jet with $E_T^{\text{jet}} > 17 \text{ GeV}$ and $-1 < \eta^{\text{jet}} < 2.5$

• The measured $\langle \psi(r=0.5) \rangle$ shows **no significant variation with η^{jet}**

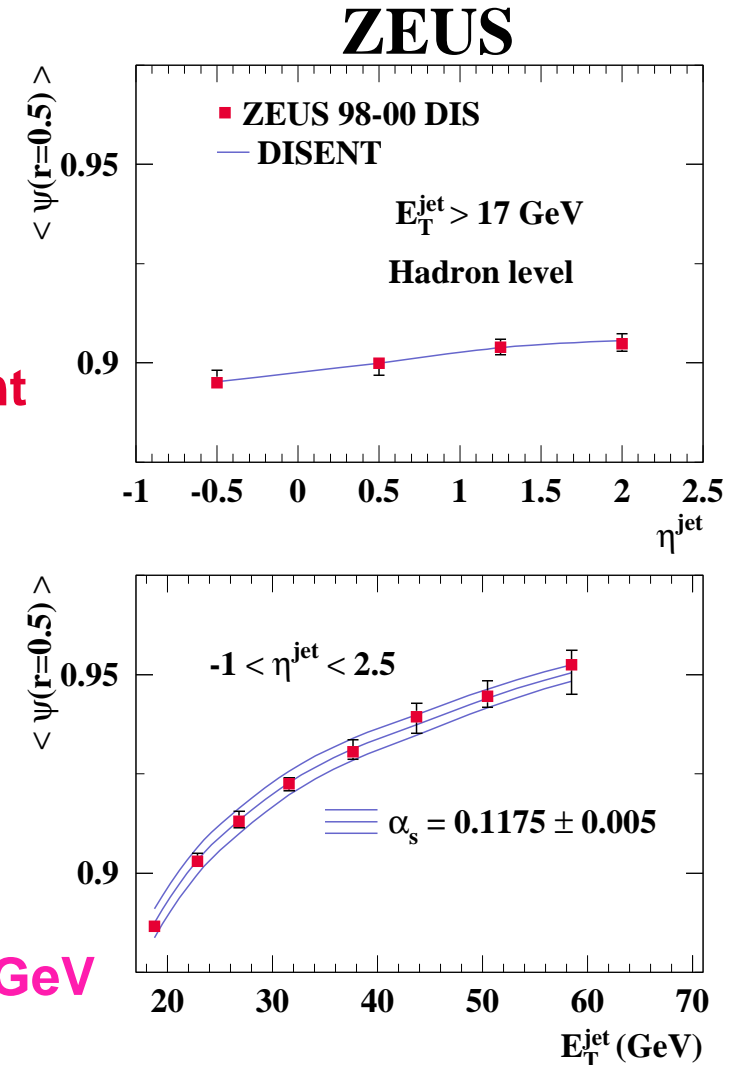
• The measured $\langle \psi(r=0.5) \rangle$ increases with E_T^{jet}
→ the jets become narrower as E_T^{jet} increases

• Comparison with NLO QCD calculations

→ the calculations provide a good description of the data and show sensitivity to the value of $\alpha_s(M_Z)$

• From the measured $\langle \psi(r=0.5) \rangle$ for $E_T^{\text{jet}} > 21 \text{ GeV}$ a value of $\alpha_s(M_Z)$ has been extracted:

$$\alpha_s(M_Z) = 0.1176 \pm 0.0009 \text{ (stat.) } \begin{matrix} +0.0009 \\ -0.0026 \end{matrix} \text{ (exp.) } \begin{matrix} +0.0091 \\ -0.0072 \end{matrix} \text{ (th.)}$$

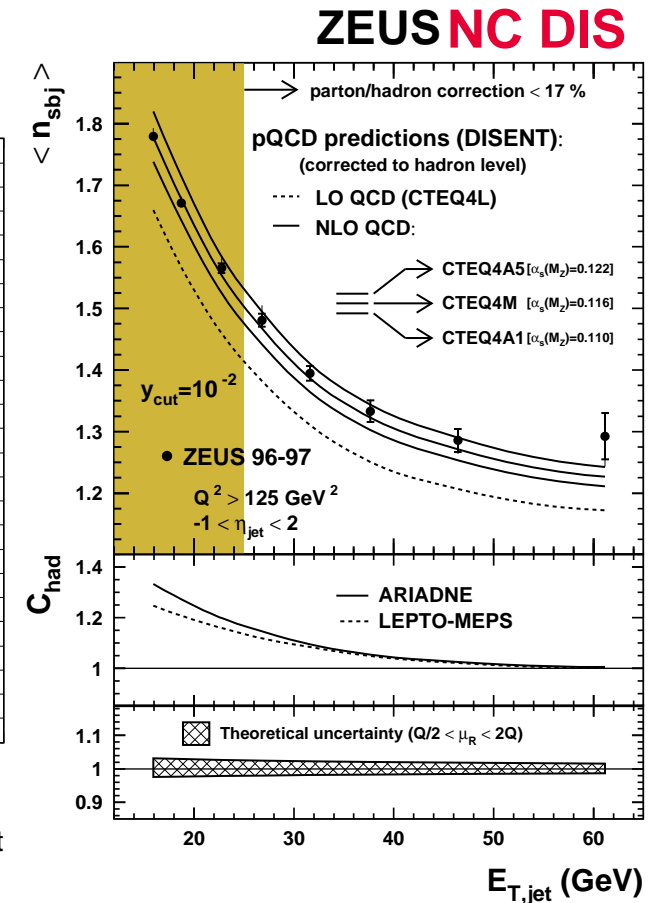
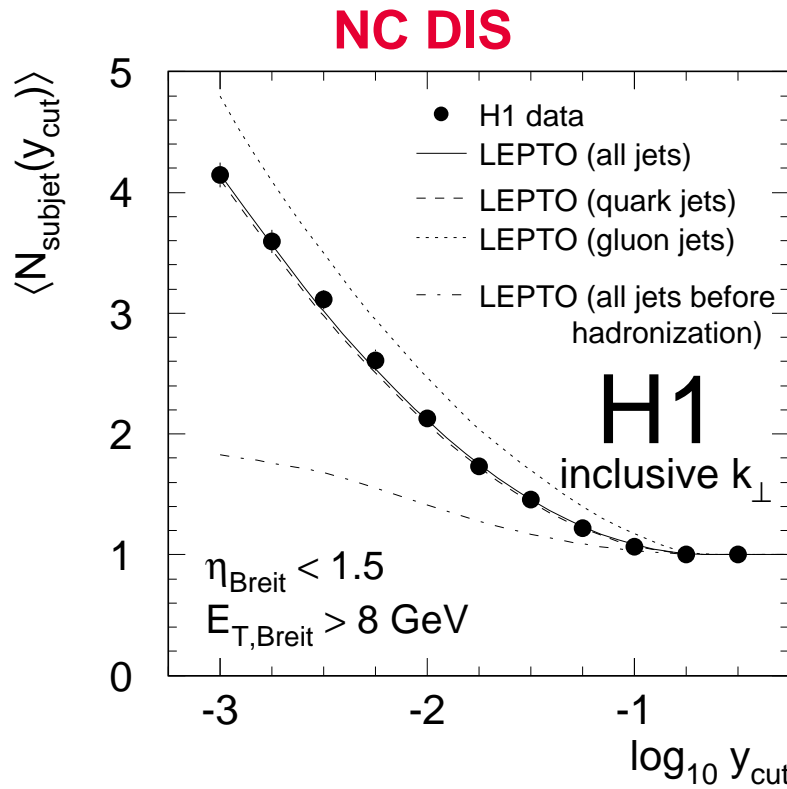
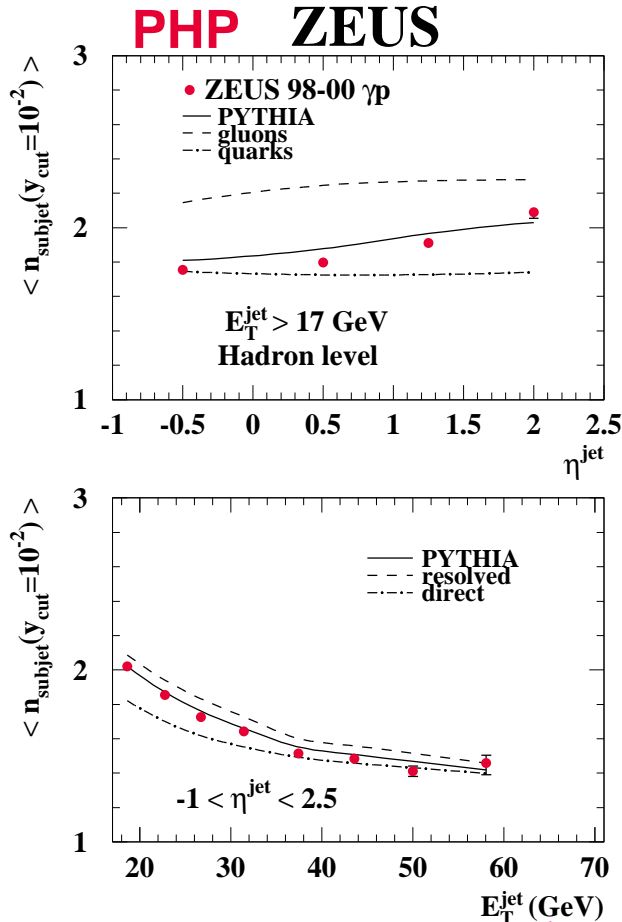




Mean subjet multiplicity in photoproduction and NC DIS



- y_{cut} , η^{jet} and E_T^{jet} dependence of $\langle \psi(r=0.5) \rangle$ in photoproduction and NC DIS:
 - same conclusions as for the integrated jet shape

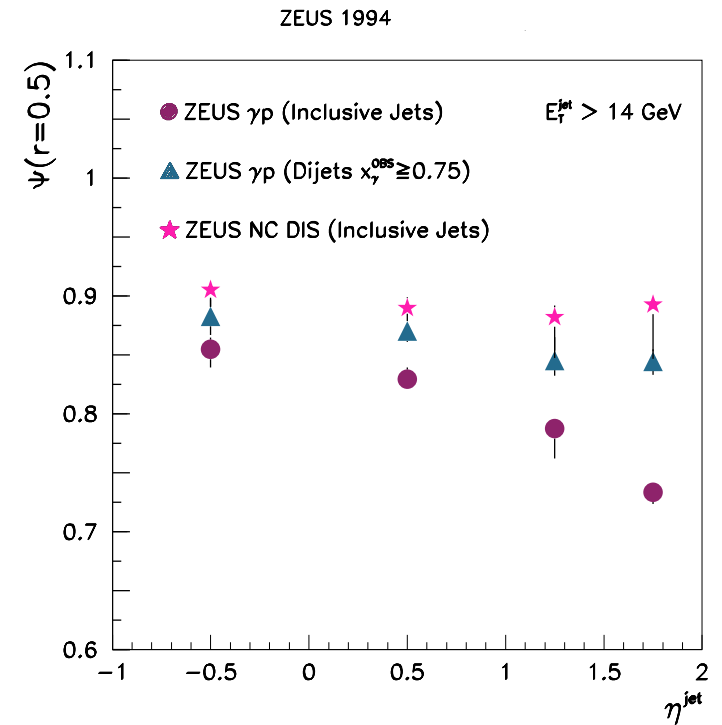
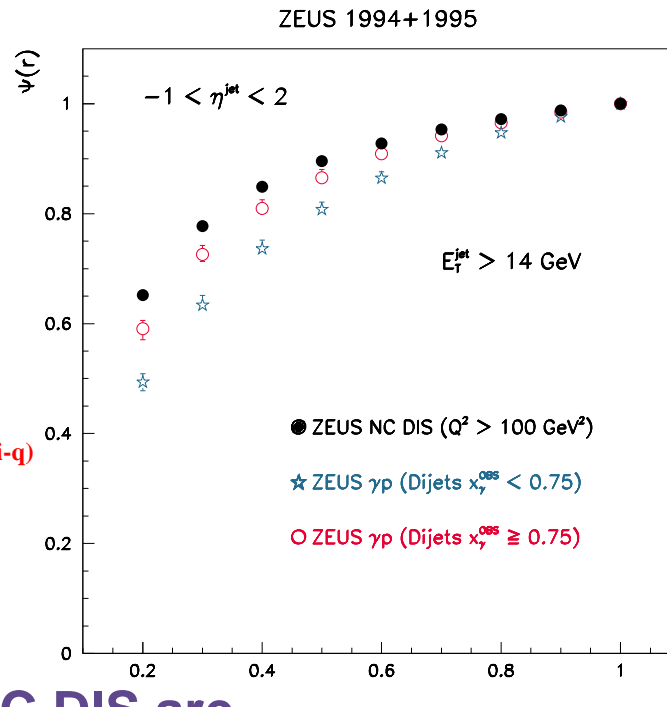
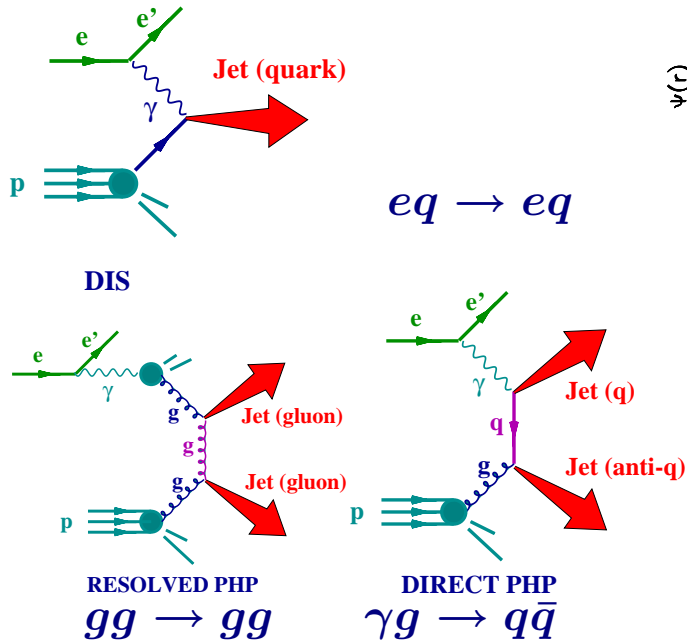


- From the measured $\langle n_{sbj}(y_{cut} = 10^{-2}) \rangle$ for $E_T^{jet} > 25$ GeV a value of $\alpha_s(M_Z)$ has been extracted:

$$\alpha_s(M_Z) = 0.1187 \pm 0.0017 \text{ (stat.) } \begin{matrix} +0.0024 \\ -0.0009 \end{matrix} \text{ (exp.) } \begin{matrix} +0.0093 \\ -0.0076 \end{matrix} \text{ (th.)}$$

Jet properties in different environments

Comparison of jet shapes in photoproduction and NC DIS



● r dependence: jets in NC DIS are

- narrower than in γp with $x_{\gamma}^{\text{obs}} < 0.75$ → resolved dominated by gluon jets
- similar to γp with $x_{\gamma}^{\text{obs}} > 0.75$ → direct dominated by quark jets

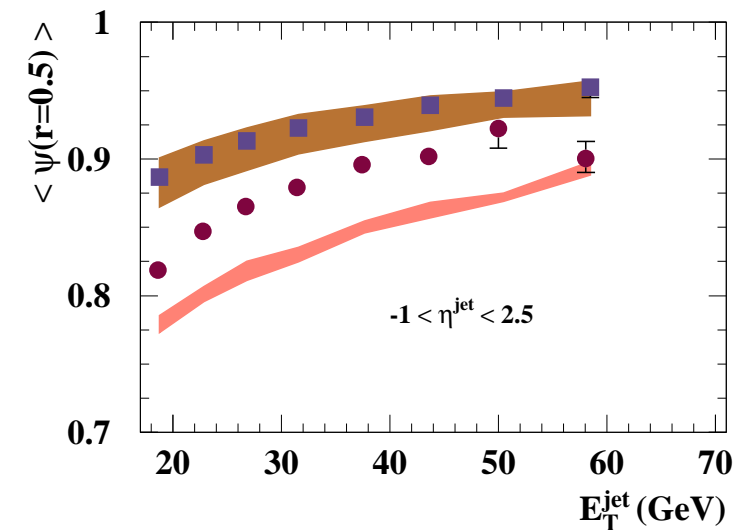
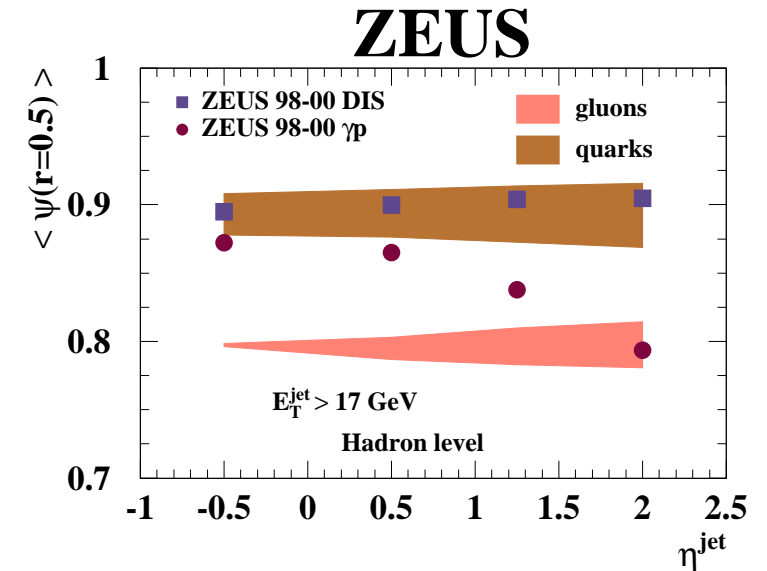
● η^{jet} dependence:

- inclusive jets in γp : the fraction of gluons increases as η^{jet} increases
- γp with $x_{\gamma}^{\text{obs}} > 0.75$ } — mainly quarks
- inclusive jets in DIS } — no η^{jet} dependence

Comparison of jet shapes in photoproduction and NC DIS



- η^{jet} dependence:
 - DIS: no significant dependence
 - γp : jets become broader as η^{jet} increases
- Comparison with QCD:
 - DIS: consistent with being dominated by quark-initiated jets
 - γp : broadening of data consistent with increase of fraction of gluon-initiated jets
- E_T^{jet} dependence:
 - DIS and γp : jets become narrower as E_T^{jet} increases



Comparison of subjet multiplicities in NC and CC DIS



• E_T^{jet} and Q^2 dependence of $\langle n_{\text{subj}}(y_{\text{cut}} = 10^{-2}) \rangle$ in CC DIS

– Jets searched using the k_T cluster algorithm in LAB frame

– Kinematic region: $Q^2 > 200 \text{ GeV}^2$ and $y < 0.9$

– At least one jet with $E_T^{\text{jet}} > 14 \text{ GeV}$ and $-1 < \eta^{\text{jet}} < 2$

• The measured $\langle n_{\text{subj}}(y_{\text{cut}} = 10^{-2}) \rangle$ decreases with E_T^{jet} or Q^2

→ jets get narrower as E_T^{jet} or Q^2 increase

• Comparison with NLO QCD calculations

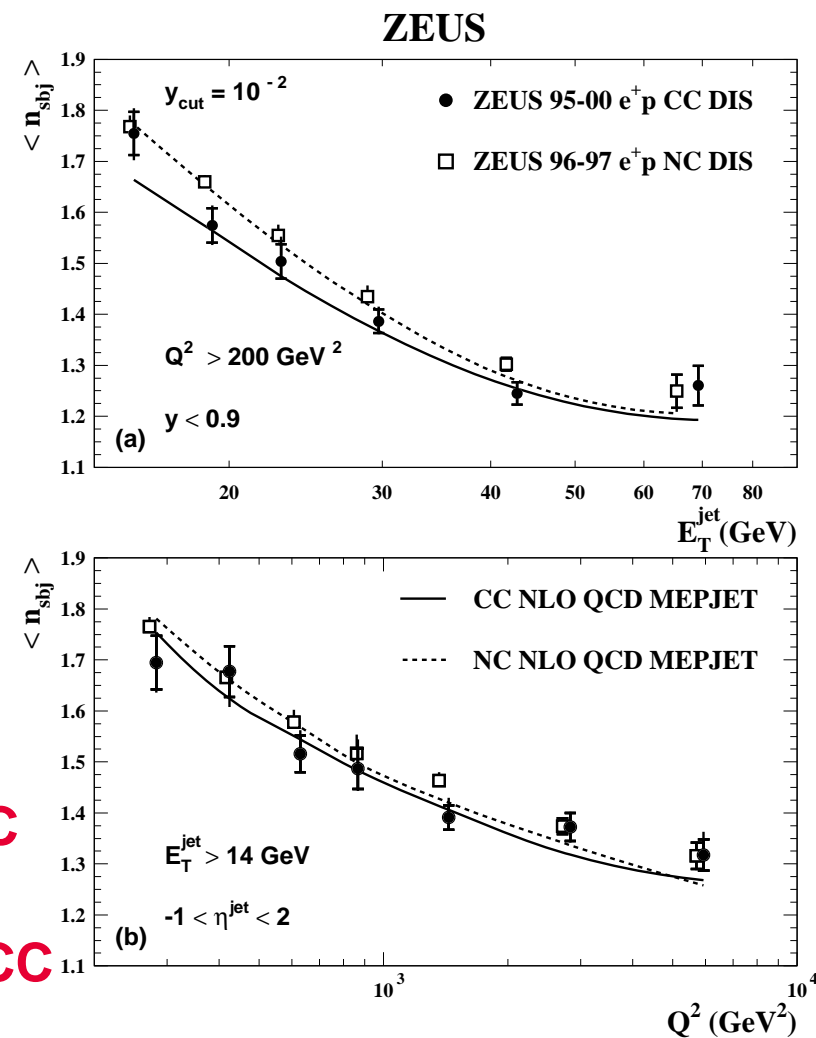
→ the calculations provide a good description of the data

• Comparison with NC DIS data

→ E_T^{jet} dependence: $\langle n_{\text{subj}} \rangle$ slightly larger in NC than in CC

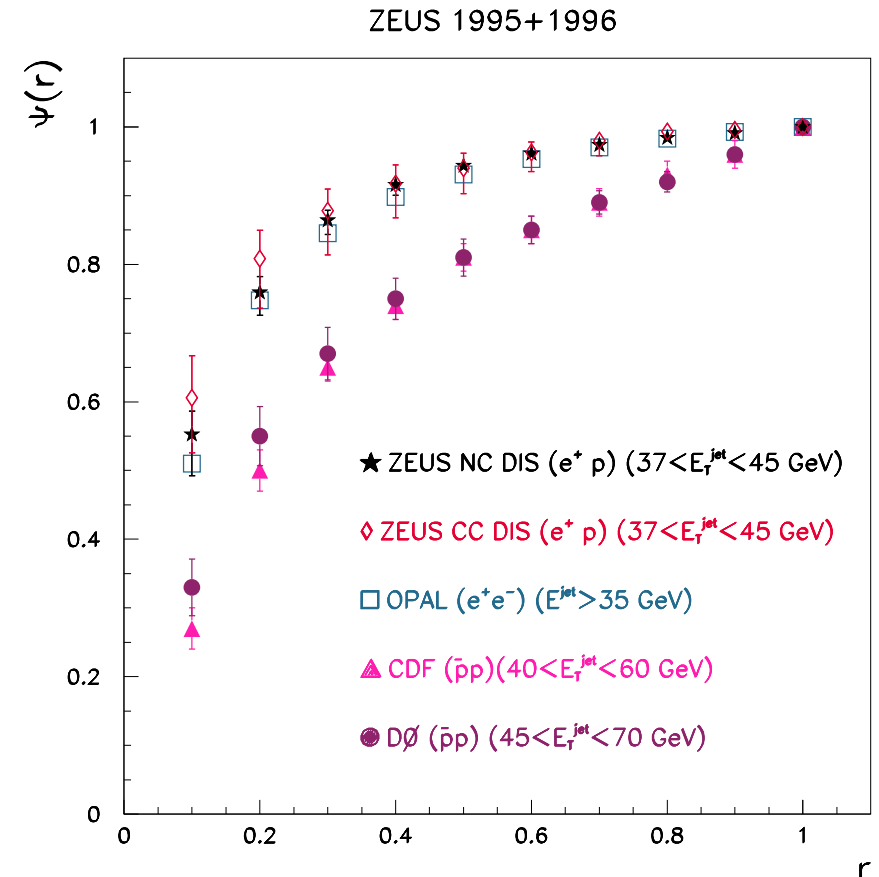
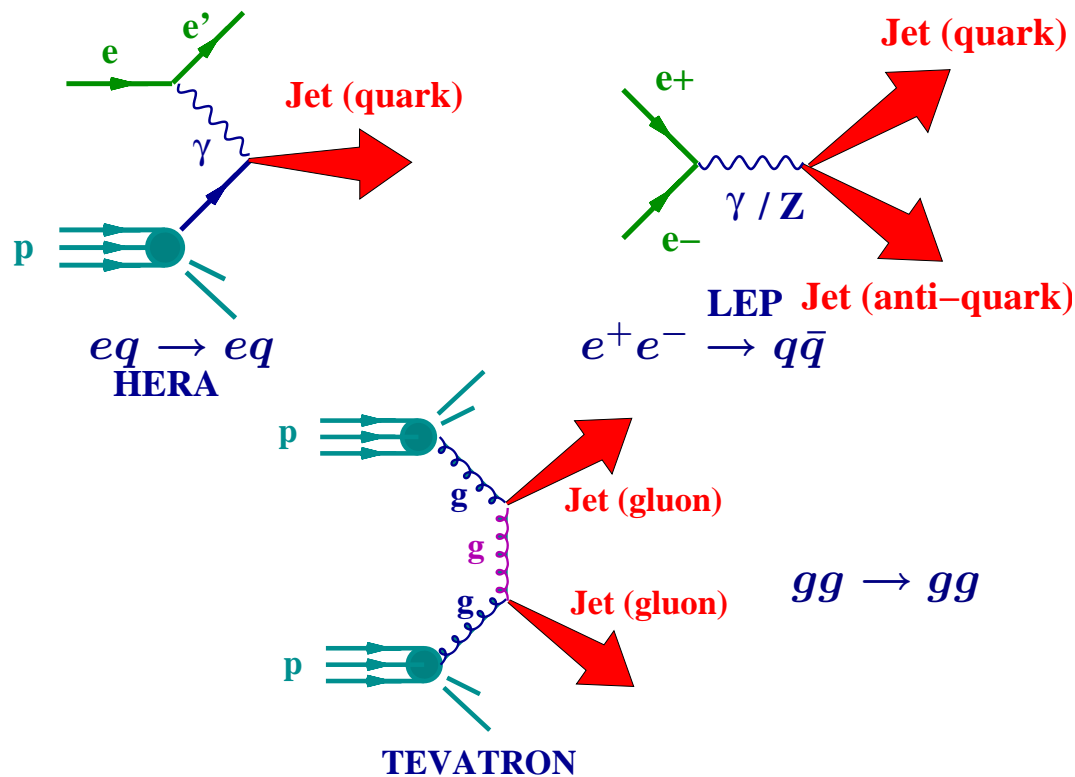
→ Q^2 dependence of $\langle n_{\text{subj}} \rangle$ similar in NC and CC

→ differences in E_T^{jet} dependence can be attributed to different Q^2 spectra in NC and CC



ZEUS Collab, EPJ C 31 (2003) 149

Comparison of jet shapes in ep , e^+e^- and $p\bar{p}$



- **Jets in ep and e^+e^- are:**

- similar: jets in ep and e^+e^- come predominantly from quarks
- pattern of QCD radiation within a quark jet is to a large extent independent of hard scattering process
- narrower than those in $p\bar{p}$: jets in $p\bar{p}$ come predominantly from gluons

Quark and gluon jets properties

Identification of quark and gluon jets

- Charm photoproduction provides a handle to identify quark and gluon jets by selecting dijet events with one jet tagged as the **charmed jet** and measuring the substructure of the **other (“untagged”) jet in the event: enriched and unbiased sample of charm jets**

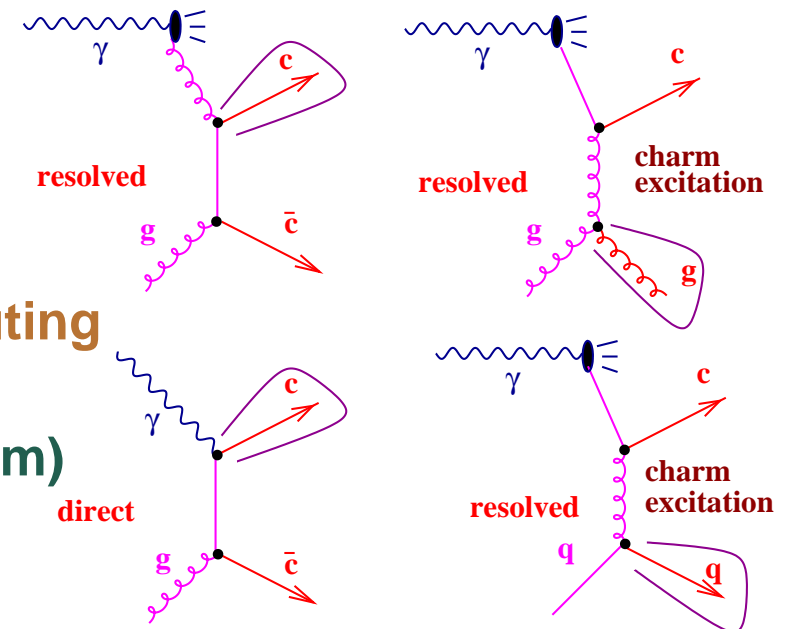
- **In photoproduction:**

- in direct processes, the “untagged” jet is also a charm quark

- in resolved processes, there are several contributing processes:

- gluon-gluon fusion (“untagged” jet: also charm)

- charm-excitation processes (“untagged” jet: gluon or quark)



Substructure of quark and gluon jets



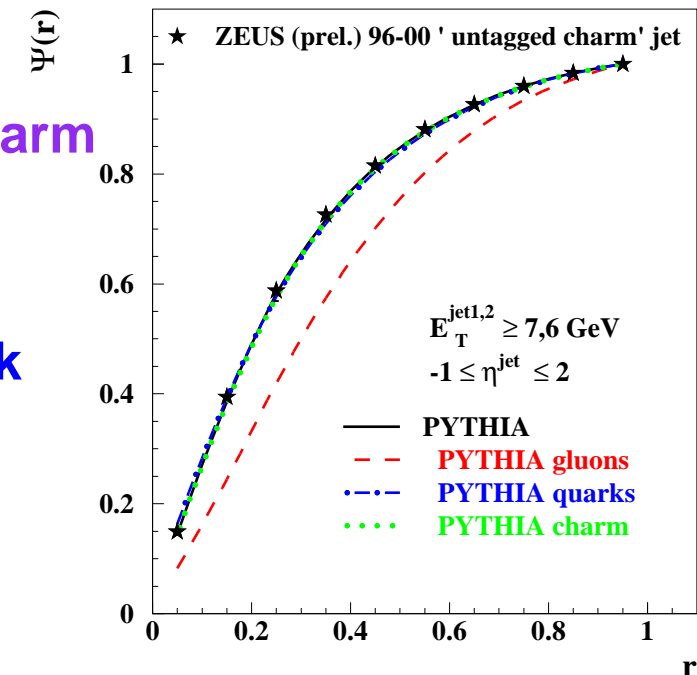
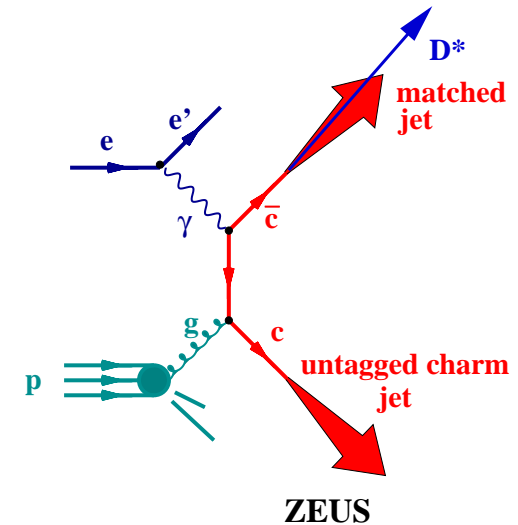
● $\langle \psi(r) \rangle$ in photoproduction with charm jets

- Jets searched using the k_T cluster algorithm
- Kinematic region: $0.2 < y < 0.85$ and $Q^2 \leq 1 \text{ GeV}^2$
- At least two jets with $E_T^{\text{jet}} > 7, 6 \text{ GeV}$ and $-1 < \eta^{\text{jet}} < 2$

● Subsample of dijet events with a $D^{*\pm}$ meson matched to one of the jets

● The other jet in the event (“untagged” charm jet) provides an enriched and unbiased sample of charm jets

→ Model predictions for charm jets and light-quark jets describe the data well



ZEUS preliminary 2001

Substructure of quark and gluon jets



● Characterization of the substructure of gluon jets:

→ extraction of $\mathcal{O}_{\text{gluon}}$ from

$$\mathcal{O}_{\text{dijet}} = f_q \cdot \mathcal{O}_{\text{quark}} + f_g \cdot \mathcal{O}_{\text{gluon}}$$

→ $\mathcal{O}_{\text{dijet}}$ is the measured observable

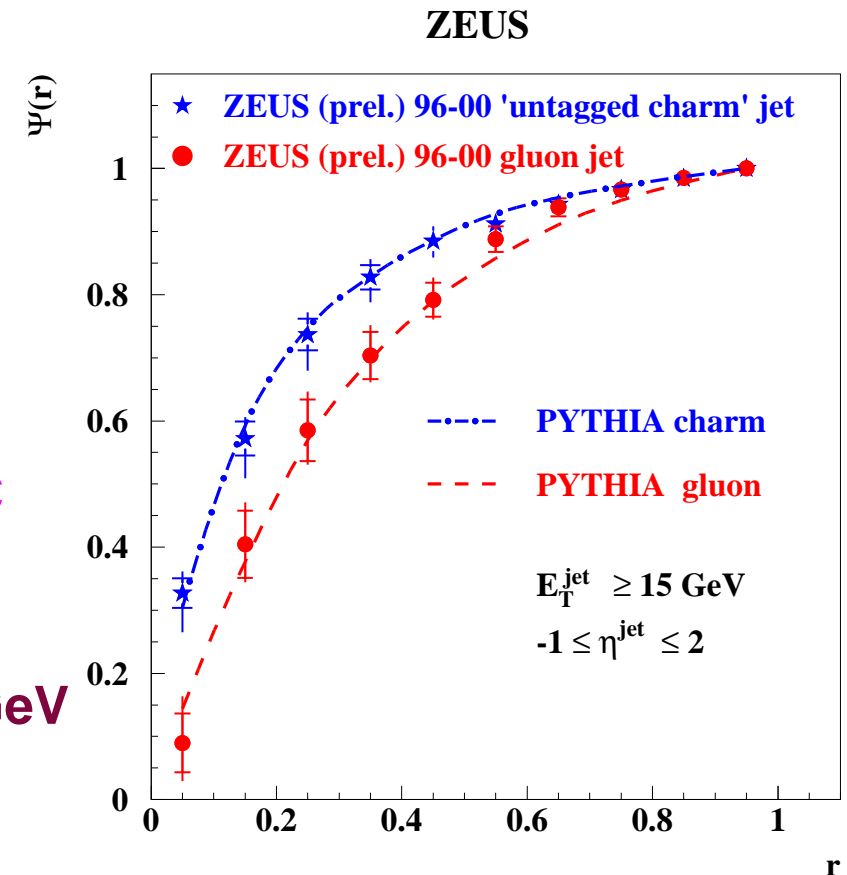
→ $\mathcal{O}_{\text{quark}}$ is approximated by $\mathcal{O}_{\text{charm}}$

→ f_q ($f_g = 1 - f_q$) is estimated using the MC models

● Extraction of gluon properties for $E_T^{\text{jet}} > 15 \text{ GeV}$

→ gluon jets are broader than quark jets

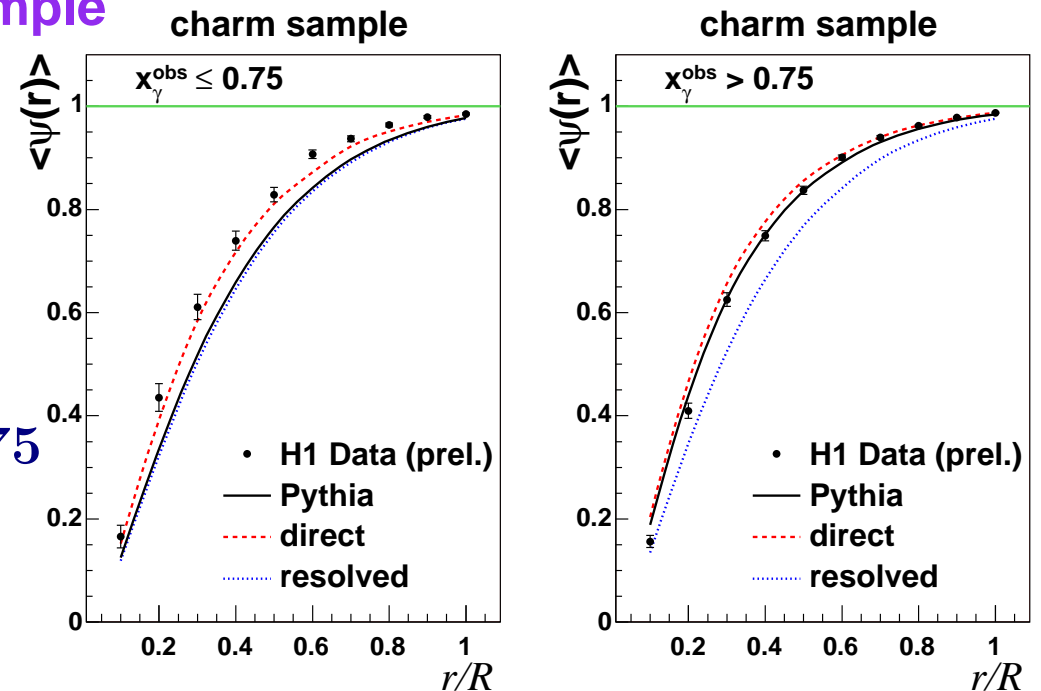
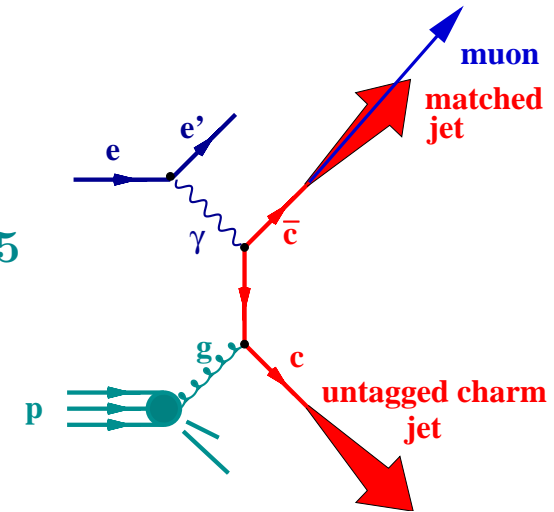
→ Model predictions for quark and gluon jets describe the measurements well





Substructure of quark and gluon jets

- $\langle \psi(r) \rangle$ in photoproduction with charm jets
 - Jets searched using the k_T cluster algorithm
 - Kinematic region: $0.2 < y < 0.8$ and $Q^2 \leq 1 \text{ GeV}^2$
 - At least two jets with $E_T^{\text{jet}} > 7, 6 \text{ GeV}$ and $-0.75 < \eta^{\text{jet}} < 1.5$
- Subsample of dijet events with a μ matched to one of the jets
- The other jet in the event (“untagged” charm jet) provides an enriched and unbiased sample of charm jets
 - purity of the tagged jet: 71 – 73%
- The predictions of PYTHIA (including charm-excitation) describe the data well for $x_\gamma^{\text{obs}} > 0.75$
- Differences are observed for $x_\gamma^{\text{obs}} \leq 0.75$
 - the data suggest a smaller fraction of gluon jets at low x_γ^{obs} than predicted by PYTHIA

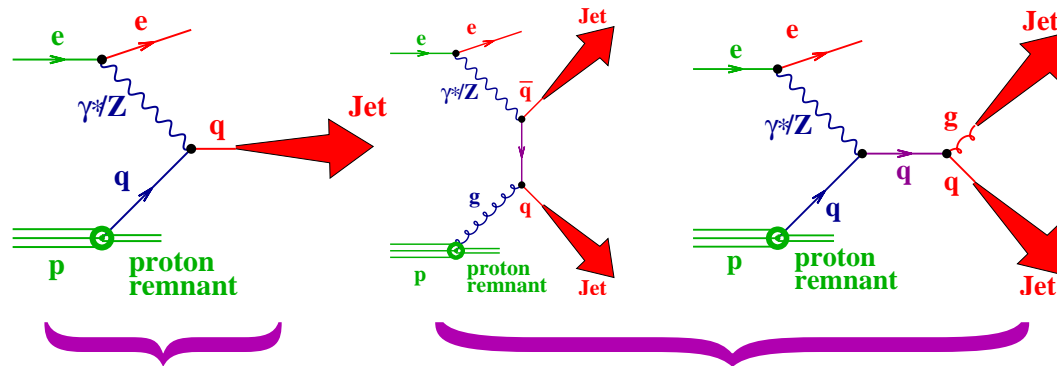


H1 Collab, H1-prelim-05-077



Substructure of quark and gluon jets

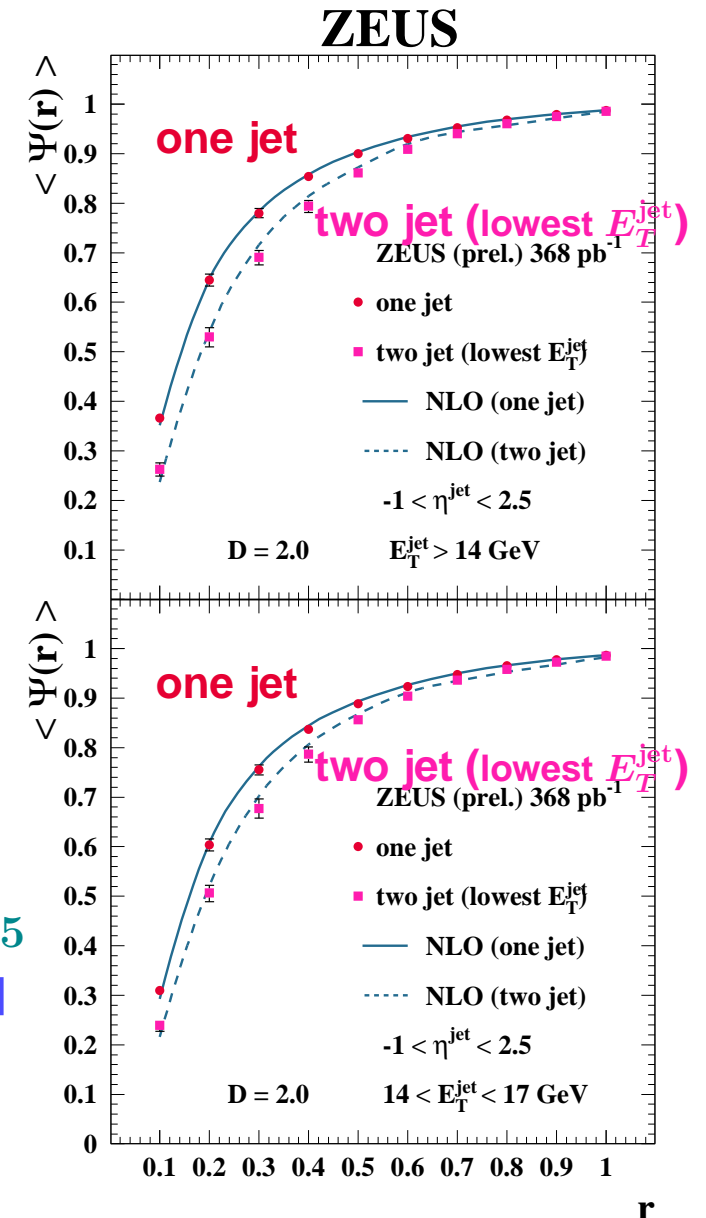
- Differences between quark and gluon jets were investigated by exploiting the different type of parton content in the final state for one-jet and dijet events in NC DIS in LAB frame



one-jet events enriched in quark jets

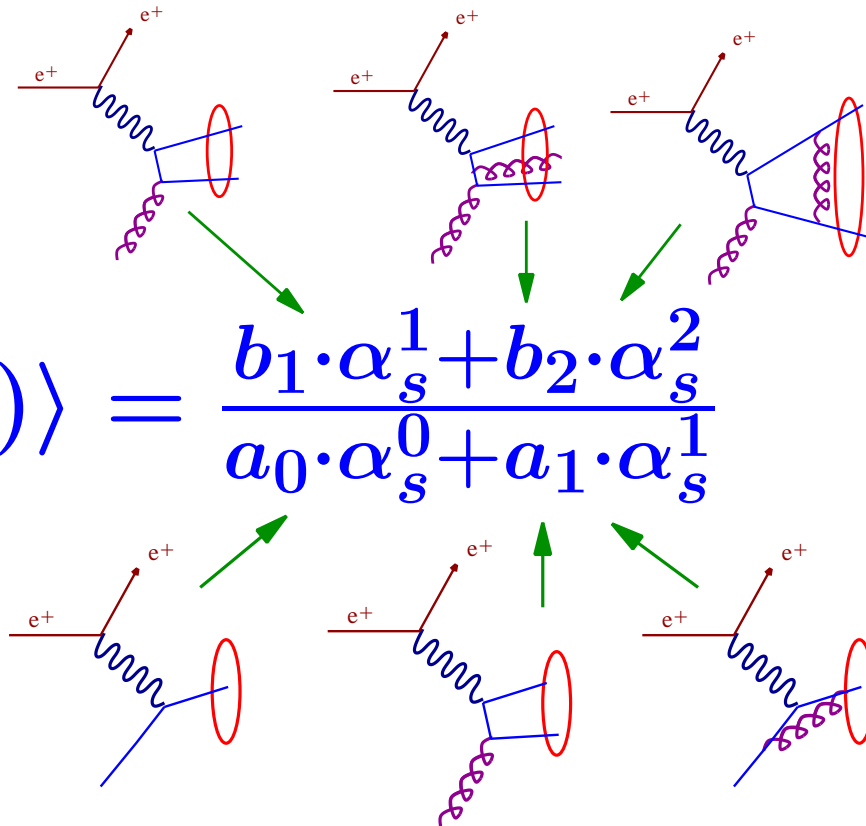
two-jet events higher content of gluon jets

- Jets searched using the k_T cluster algorithm in LAB frame
- Kinematic region: $Q^2 > 125 \text{ GeV}^2$
- At least one (two) jet(s) with $E_T^{\text{jet}} > 17 \text{ GeV}$ and $-1 < \eta^{\text{jet}} < 2.5$
- In the dijet sample, the lowest- E_T^{jet} jet is considered if distance jet-jet = $\sqrt{\Delta\eta^2 + \Delta\phi^2} \leq D = 2$
- The lowest- E_T^{jet} jet in the two-jet sample is broader than the one-jet sample



ZEUS Collab, ZEUS-prel-07-013

NLO QCD calculations for one-jet production



$$\langle 1 - \Psi(r) \rangle = \frac{b_1 \cdot \alpha_s^1 + b_2 \cdot \alpha_s^2}{a_0 \cdot \alpha_s^0 + a_1 \cdot \alpha_s^1}$$

DISENT program
S. Catani and M.H. Seymour
Nucl. Phys. B485 (1997) 291

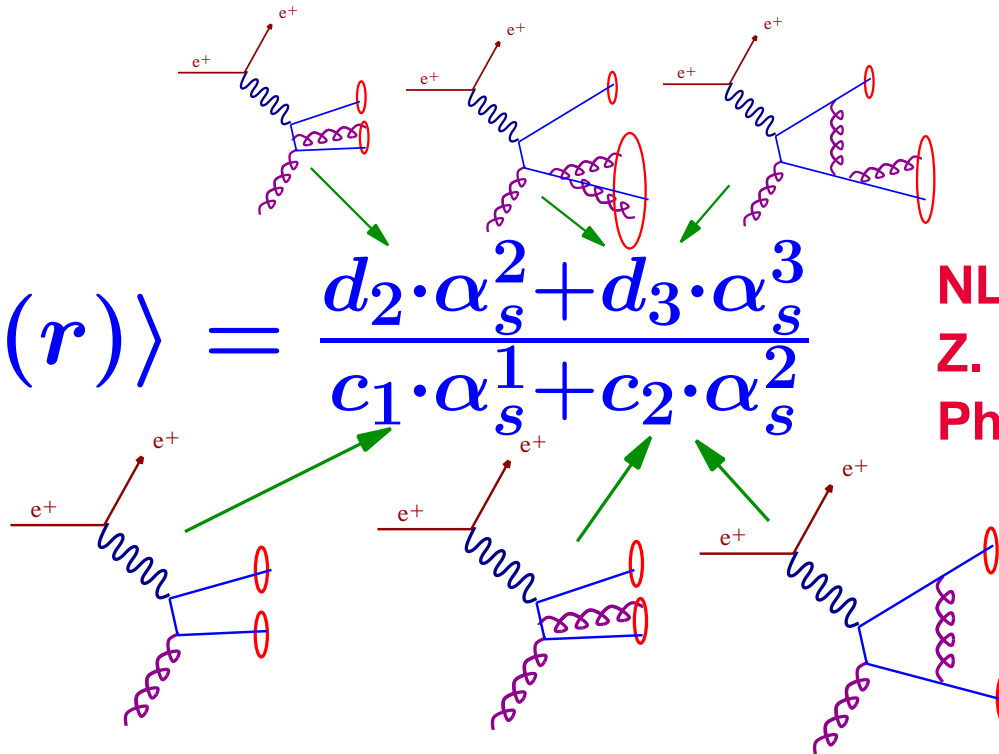
- **DISENT program:** $\alpha_s(M_Z) = 0.118$; $\mu_R = \mu_F = Q$; CTEQ6 proton PDFs
 → **Dominant theoretical uncertainty: terms beyond NLO, < 5% for $r \geq 0.2$**

NLO QCD calculations for two-jet production



$$\langle 1 - \Psi(r) \rangle = \frac{d_2 \cdot \alpha_s^2 + d_3 \cdot \alpha_s^3}{c_1 \cdot \alpha_s + c_2 \cdot \alpha_s^2}$$

NLOJET++ program
Z. Nagy and Z. Trocsanyi
Phys.Rev.Lett. 87 (2001) 082001

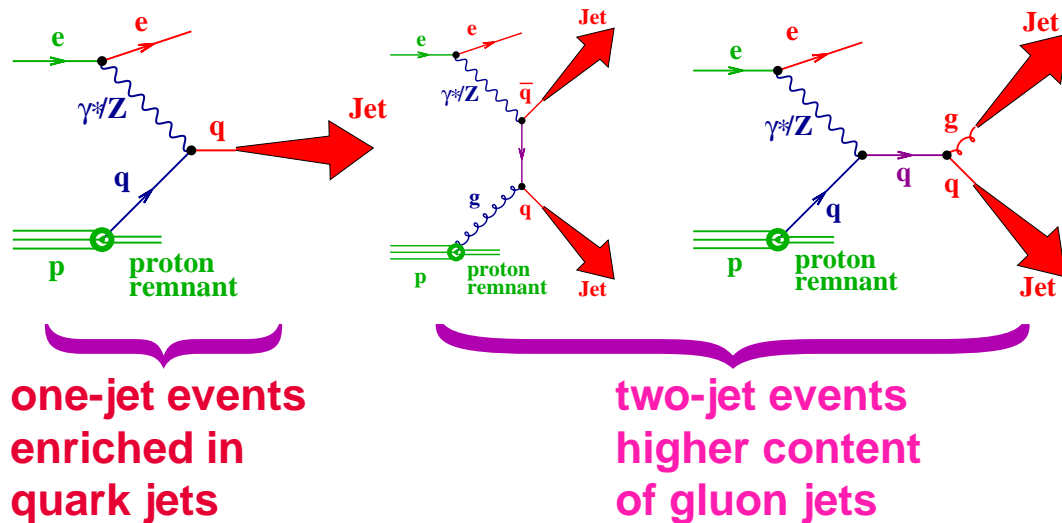


- **NLOJET++ program:** $\alpha_s(M_Z) = 0.118$; $\mu_R = \mu_F = Q$; CTEQ6 proton PDFs

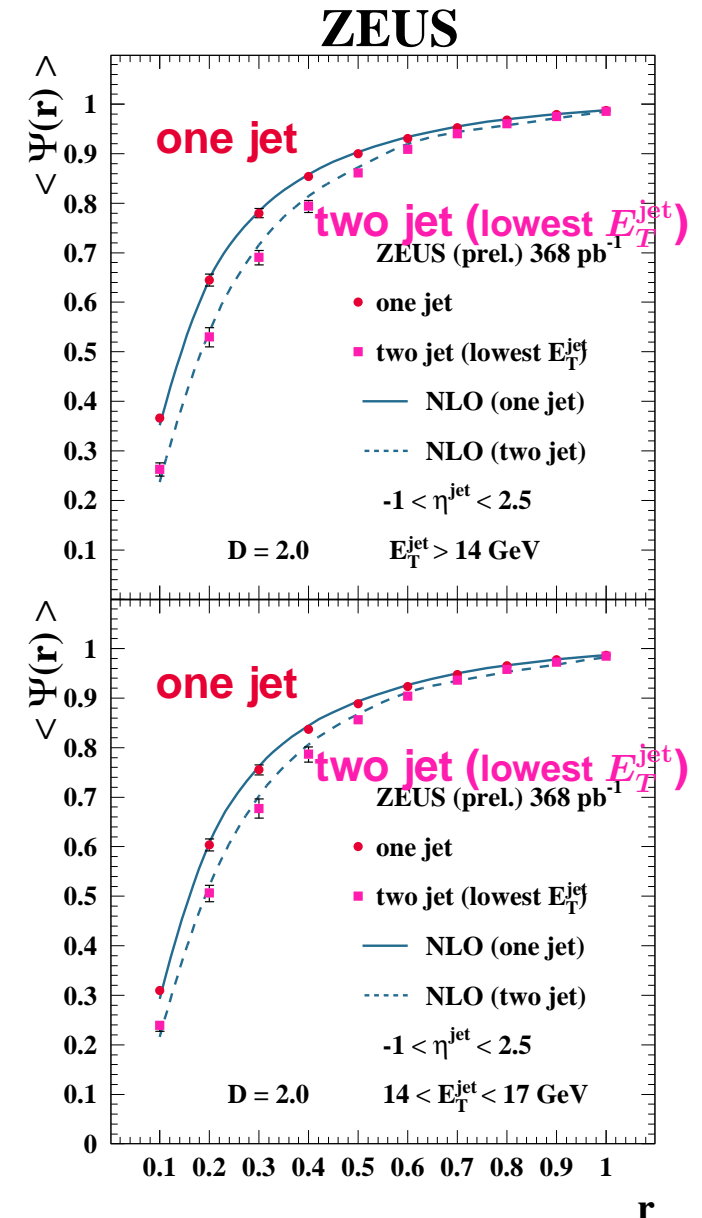


Substructure of quark and gluon jets

- Differences between quark and gluon jets were investigated by exploiting the different type of parton content in the final state for one-jet and dijet events in NC DIS in LAB frame



→ The lowest- E_T^{jet} jet in the two-jet sample is broader than the one-jet sample: consistent with a higher gluon content in dijet events, as predicted by pQCD



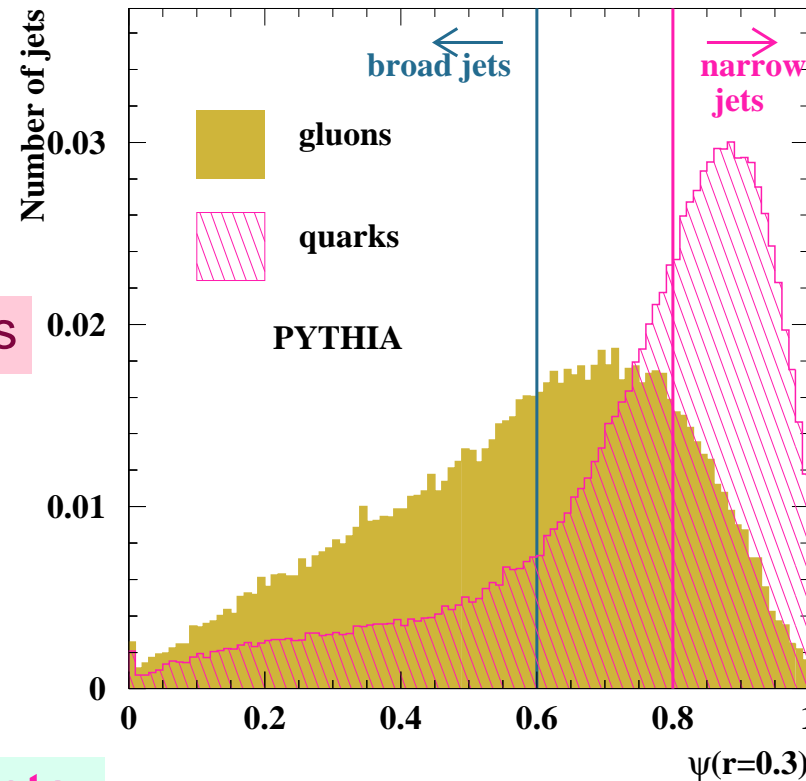
ZEUS Collab, ZEUS-prel-07-013



Identification of quark and gluon jets

- The Monte Carlo predictions of $\psi(r)$ for quark- and gluon-initiated jets show the expected differences
- Statistical identification of quark and gluon jets assuming:

ZEUS



gluon jets ↔ “broad” jets

quark jets ↔ “narrow” jets

→ Samples enriched in gluon-like (“broad”) jets:

quark-like (“narrow”) jets:

$$\psi(r = 0.3) < 0.6$$

are obtained by requiring

$$\psi(r = 0.3) > 0.8$$

Substructure dependence of jet cross sections



- $d\sigma/d\eta^{\text{jet}}$ for broad and narrow jets in photoproduction

- Jets searched using the k_T cluster algorithm

- Kinematic region: $0.2 < y < 0.85$ and

$$Q^2 \leq 1 \text{ GeV}^2$$

- At least one jet with $E_T^{\text{jet}} > 17 \text{ GeV}$ and

$$-1 < \eta^{\text{jet}} < 2.5$$

- $d\sigma/d\eta^{\text{jet}}$ for “broad” and “narrow” jets show different shape

- Comparison with leading-logarithm parton shower MC calculations:

- * same jet-shape cuts as the data

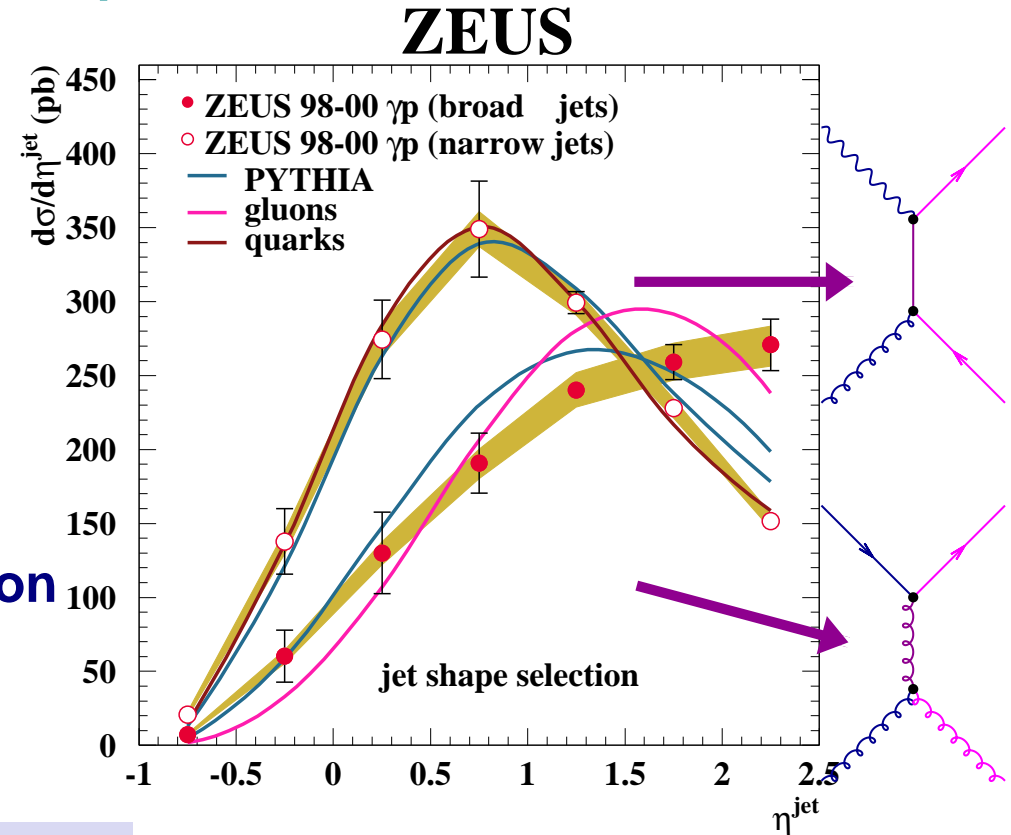
- * MC area normalised to data

- good description of the shape of the data

- Parton content of the final state from MC calculations of PYTHIA (HERWIG):

- “broad” jets: 17(15)% gg , 58(54)% gq and 25(31)% qq

- “narrow” jets: 54(56)% qq , 41(41)% qg and 5(3)% gg



Substructure dependence of jet cross sections



- $d\sigma/d|\cos\theta^*|$ for samples of two “broad”-jet events and two “narrow”-jet events exhibit a different slope:

* data and MC normalised to unity at $|\cos\theta^*| = 0.1$

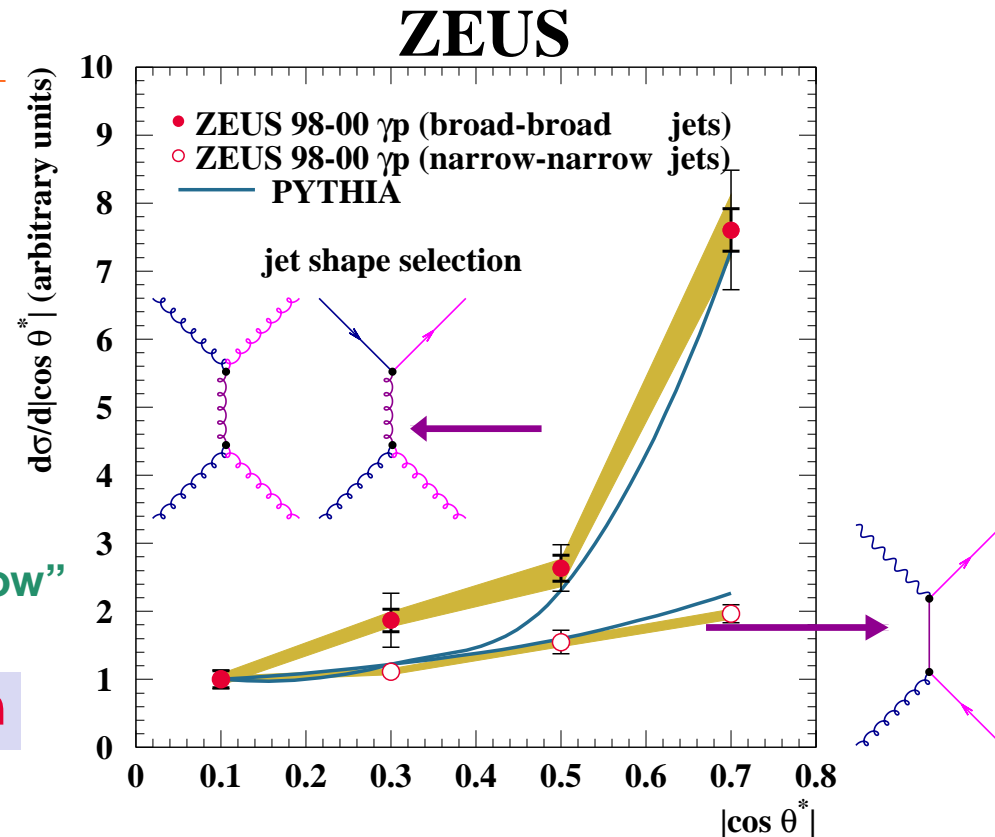
→ $d\sigma/d|\cos\theta^*|$ at $|\cos\theta^*| = 0.7$ for “broad-broad” (“narrow-narrow”) events is more than seven (only two) times larger than at 0.1

- Comparison with MC:

* same selection cuts as the data for “broad”/“narrow” sample

→ PYTHIA gives a reasonable description of the shape of the data

→ Different slope understood in terms of the dominant two-body processes: $qg \rightarrow qg$ (dominant in “broad-broad” sample) rises more steeply than $\gamma g \rightarrow q\bar{q}$ (dominant in “narrow-narrow” sample) due to different spin of exchanged particle





Substructure dependence of jet cross sections

- $d\sigma/d\cos\theta^*$ for a sample of events with one “broad” jet and one “narrow” jet measured wrt the “broad” jet shows different behaviour on the negative and positive sides:

* data and MC normalised to unity at $\cos\theta^* = 0.1$

→ $d\sigma/d\cos\theta^*$ at 0.7 is \approx two times larger than at -0.7

- Comparison with MC:

* same “broad-narrow” selection as for the data

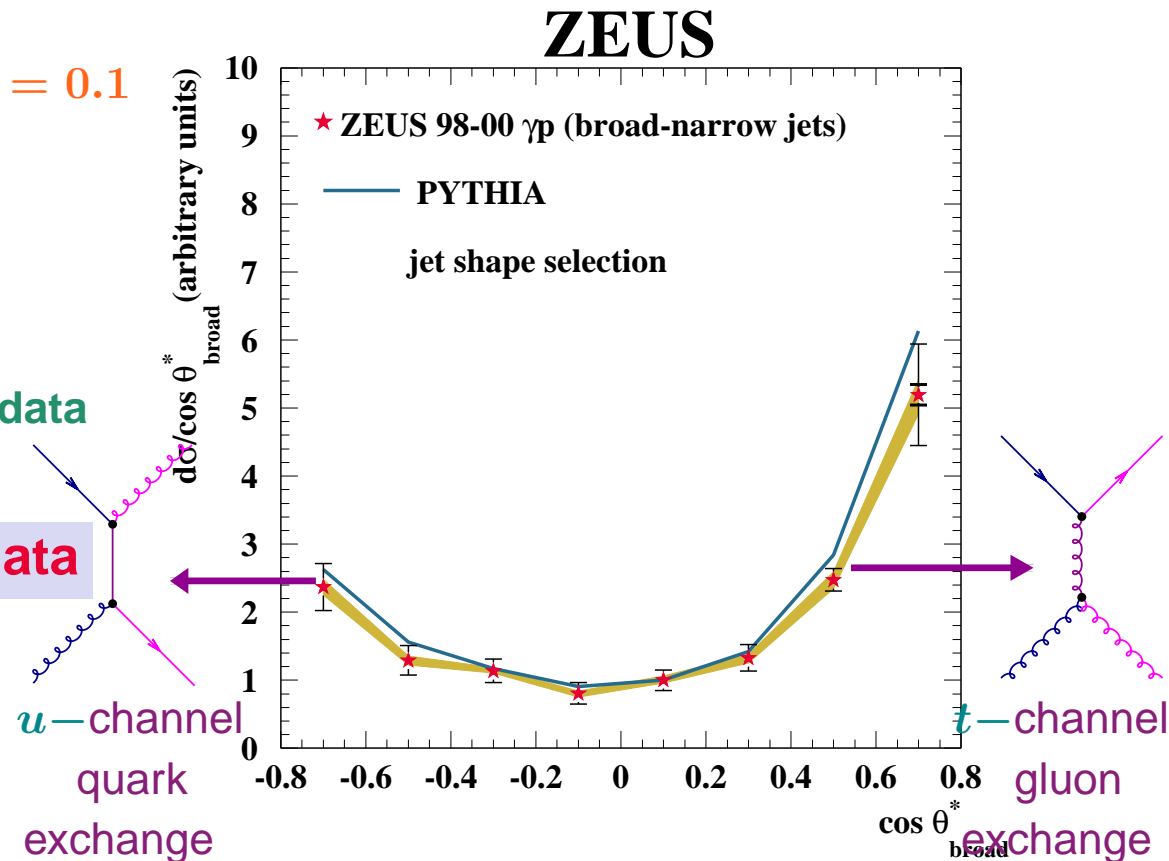
→ PYTHIA gives a reasonable description of the shape of the data

→ Observed asymmetry understood in terms of the dominant resolved subprocess: $q\gamma g_p \rightarrow qg$

→ The asymmetry is due to the different dominant diagrams for $\cos\theta^* \rightarrow \pm 1$:

* t -channel gluon exchange at $\cos\theta^* = +1$

* u -channel quark exchange at $\cos\theta^* = -1$



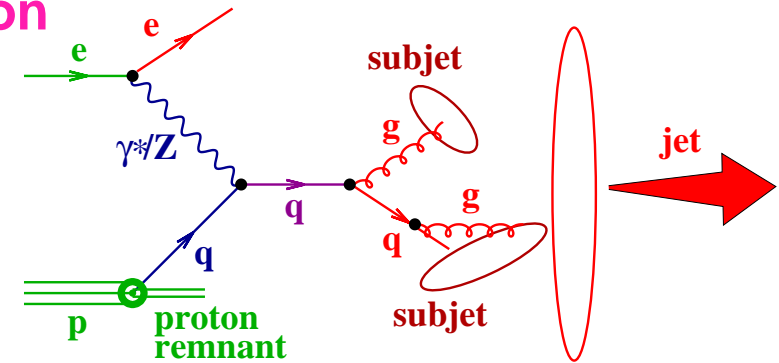
Pattern of parton radiation

Subject distributions



- Subject distributions can be used to study:

- pattern of parton radiation from a primary parton
 - direct test of splitting functions $P_{ab}(z, \mu)$ and their scale dependence
- colour coherence
 - soft gluon radiation tends to be emitted towards proton direction

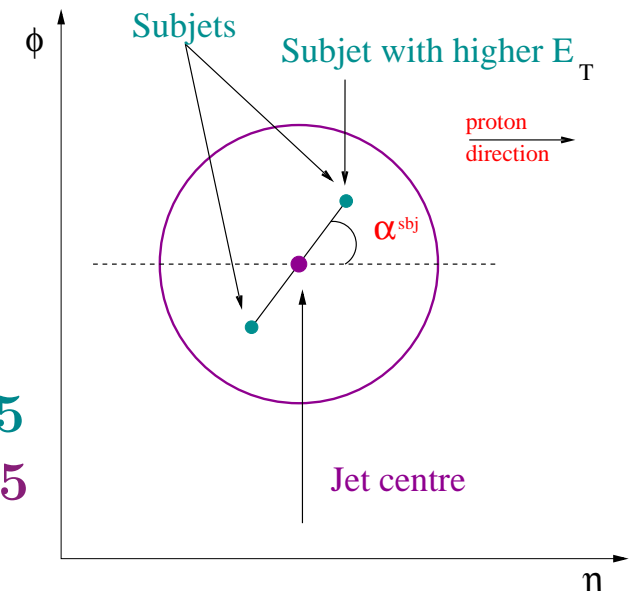


- Measurements of normalised cross sections as functions of

$$E_T^{\text{sbj}} / E_T^{\text{jet}}, \eta^{\text{sbj}} - \eta^{\text{jet}}, |\phi^{\text{sbj}} - \phi^{\text{jet}}| \text{ and } \alpha^{\text{sbj}}$$

and their dependence with E_T^{jet} , Q^2 and x

- Jets searched using the k_T cluster algorithm in LAB frame
- Kinematic region: $Q^2 > 125 \text{ GeV}^2$
- At least one jet with $E_T^{\text{jet}} > 14 \text{ GeV}$ and $-1 < \eta^{\text{jet}} < 2.5$
- Final sample: jets that have two subjects for $y_{\text{cut}} = 0.05$



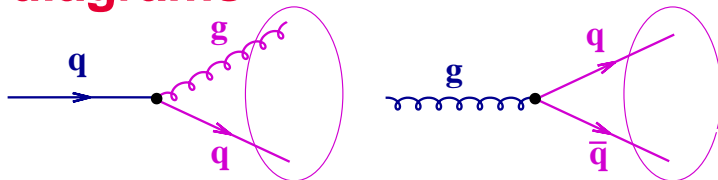


Subjet distributions

● Normalised subjet cross sections compared with NLO calculations:

- E_T^{sbj} / E_T^{jet} : the two subjets tend to have similar E_T^{sbj}
- $\eta^{sbj} - \eta^{jet}$: asymmetric two-peak structure
- $|\phi^{sbj} - \phi^{jet}|$: suppression around 0 because the two subjets cannot be resolved when close
- α^{sbj} : higher E_T^{sbj} subjet tends to be in rear direction
 → consistent with asymmetric peaks of $\eta^{sbj} - \eta^{jet}$

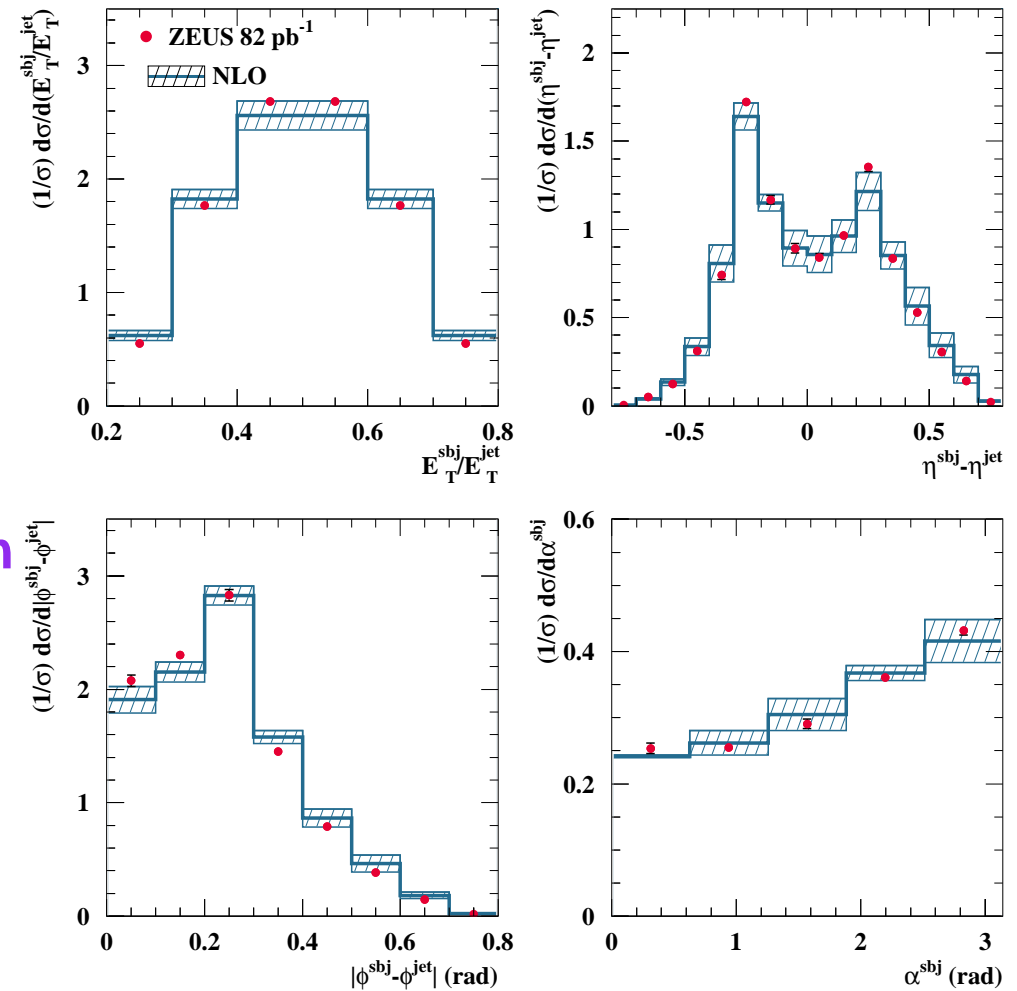
→ The NLO predictions, which contain these diagrams



describe the data adequately

ZEUS Collab, 2008

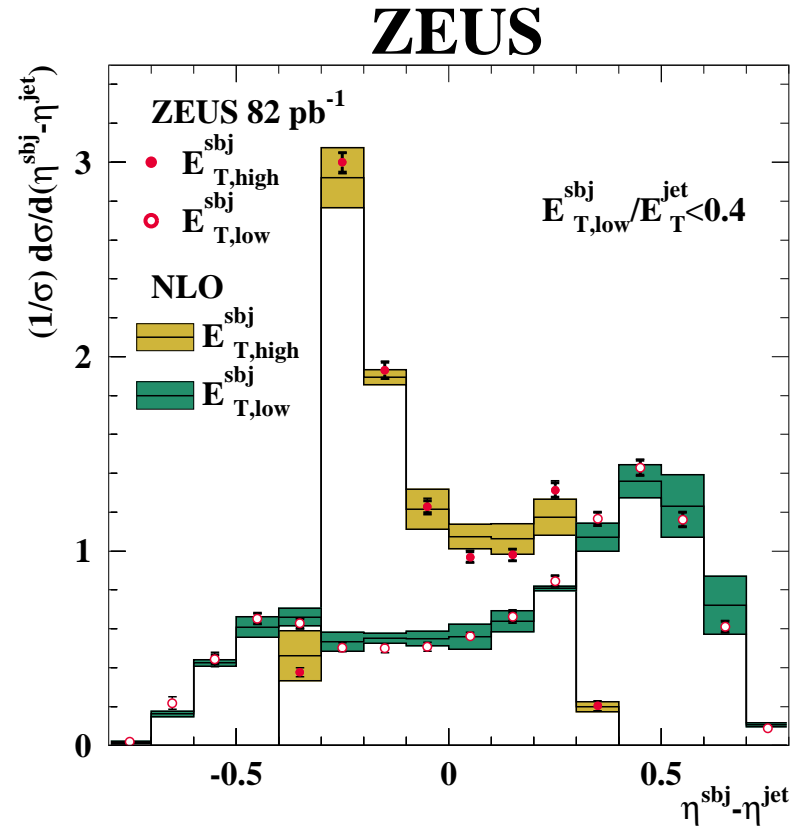
ZEUS



Subjet distributions



- $\eta^{\text{sbj}} - \eta^{\text{jet}}$ normalised cross section for $E_{T,\text{low}}^{\text{sbj}}/E_T^{\text{jet}} < 0.4$

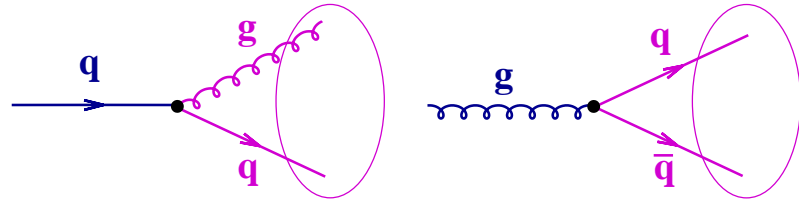


- The higher (lower) E_T^{sbj} subjet tends to be in the rear (forward) direction
- colour-coherence effects between the initial and final states
- subjet with lower E_T^{sbj} emitted predominantly towards proton beam direction

Subjet distributions



● Comparison with predictions for quark- and gluon-induced processes



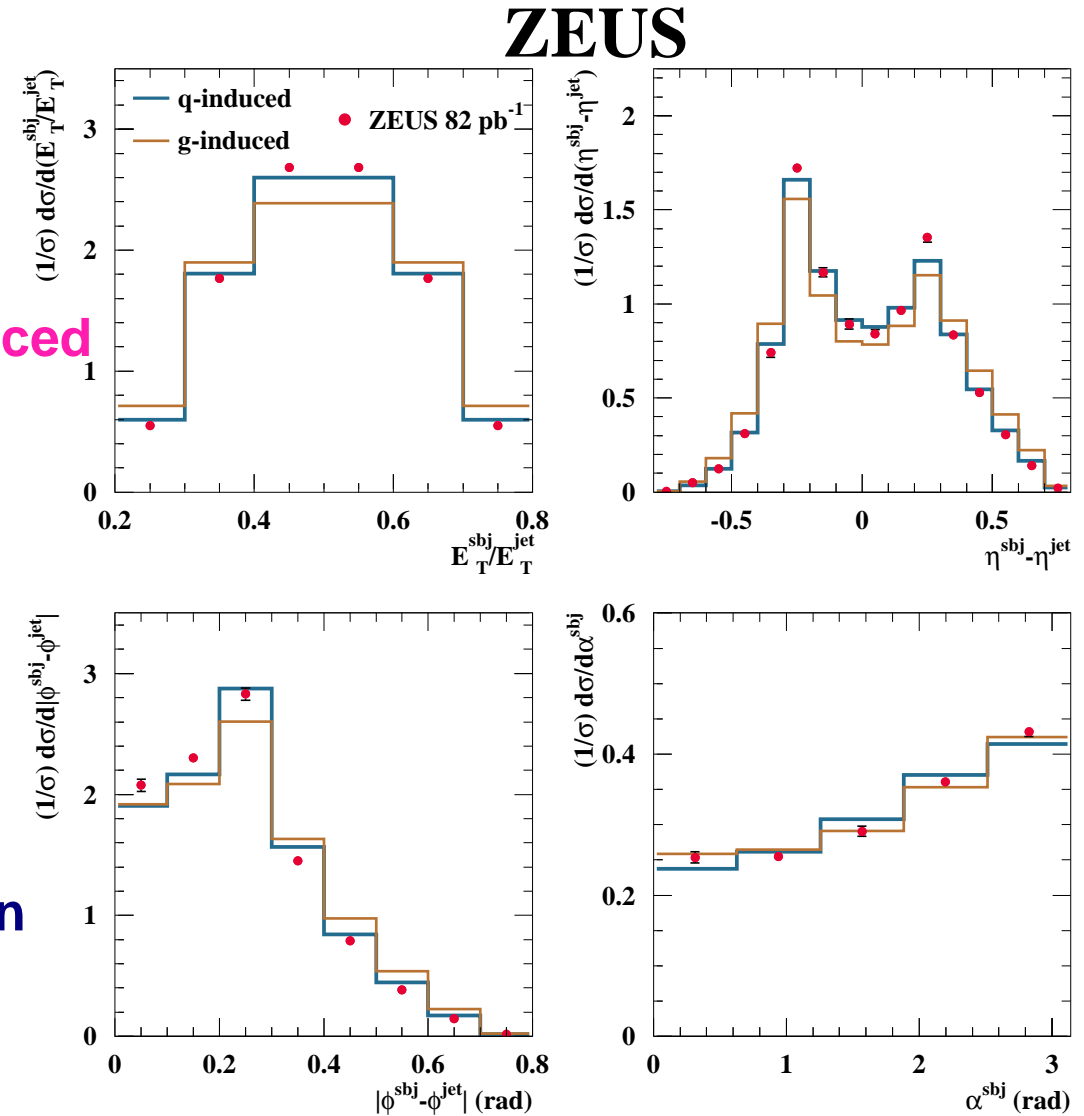
→ **NLO prediction:**

81% of q-induced and 19% of g-induced

● Predictions for these two types of processes are different:

- the two subjets in q-induced have more similar E_T^{sbj} and are closer to each other than in g-induced

→ **The data are better described by the calculations for jets arising from the splitting of a quark into a quark-gluon pair**



ZEUS Collab, 2008



Conclusions



- **Jet substructure has been extensively studied at HERA in terms of jet shapes and subjet multiplicities and distributions in DIS and photoproduction**

- **Measurements allowed**
 - ~> **stringent tests of pQCD directly beyond LO**
 - ~> **comparison of quark- and gluon-jet properties**
 - ~> **comparison of pattern of QCD radiation in different hard scattering processes**
 - ~> **determinations of $\alpha_s(M_Z)$**
 - ~> **study of underlying subprocess dynamics**
 - ~> **study of pattern of parton radiation**

↪ **Jet substructure: a powerful tool to test QCD**